Design and Optimization of Flyer

By

Ramakant I. Panchal
(10MMCC08)

DEPARTMENT OF MECHANICAL ENGINEERING
INSTITUTE OF TECHNOLOGY
NIRMA UNIVERSITY
AHMEDABAD-382481

MAY 2012

Design and Optimization of Flyer

Major Project

Submitted in partial fulfillment of the requirements

for the degree of

Master of Technology in Mechanical Engineering
(CAD/CAM)

Prepared by

Ramakant I. Panchal
(10MMCC08)

Guided by

Prof. V M Bhojawala
Prof. D V Patel

DEPARTMENT OF MECHANICAL ENGINEERING
INSTITUTE OF TECHNOLOGY
NIRMA UNIVERSITY
AHMEDABAD-382481

MAY 2012

Declaration

This is to certify that

- The thesis comprises my original work towards the degree of Master of Technology in Mechanical Engineering(CAD/CAM) at Nirma University and has not been submitted elsewhere for Degree.
- Due Acknowledgment has been made in the text to all other material used.

Ramakant I. Panchal

(10MMCC08)

Undertaking for Originality of the Work

I, **Ramakant I. Panchal**, Roll. No.**10MMCC08**, give undertaking that the Major Project entitled "**Design and Optimization of Flyer**" submitted by me, towards the partial fulfillment of the requirements for the degree of Master of Technology in Mechanical Engineering **(CAD/CAM)** of Nirma University, Ahmedabad, is the original work carried out by me and I give assurance that no attempt of plagiarism has been made. I understand that in the event of any similarity found subsequently with any published work or any dissertation work elsewhere; it will result in severe disciplinary action.

_____

Signature of Student

Date:_____

Place: NU, Ahmedabad

Endorsed by

(Signature of Guide)

Certificate

This is to certify that the Major Project entitled **"Design and Optimization of Flyer"** submitted by **Mr. Ramakant I. Panchal (Roll No: 10MMCC08)**, towards the partial fulfillment of the requirement for the degree of Master of Technology in Mechanical Engineering (CAD/CAM) of Instutite of Nirma University, Ahmedabad is the record of work carried out by him under my supervision and guidance. In my opinion, the submitted work has reached a level required for being accepted for examination. The result embodied in this major project, to the best of my knowledge, haven't been submitted to any other university or institution for award of any degree or diploma.

Prof. D V Patel
Co-Guide, Asst. Professor,
Department of Mechanical Engineering,
Institute of Technology,
Nirma University, Ahmedabad

Prof. V M Bhojawala
Guide, Asst. Professor,
Department of Mechanical Engineering,
Institute of Technology,
Nirma University, Ahmedabad

Dr R N Patel
Head and Professor,
Department of Mechanical Engineering,
Institute of Technology,
Nirma University, Ahmedabad

Dr K Kotecha
Director,
Institute of Technology,
Nirma University, Ahmedabad

Acknowledgements

With great pleasure, I wish to express my gratitude to my guide Prof. V M Bhojawala and Co-Guide Prof. D V Patel for his keen interest, constant encouragement and valuable guidance at all stages of this dissertation work.

I am very much thankful to our PG co-ordinator Dr D S Sharma, Head of Department Dr R N Patel and Director Dr K Kotecha for providing opportunity to work on this problem. I also thank Prof. A M Lakdawala for his valuable guidance.

I am thankful to all the faculty members of Mechanical Engineering Department for their expertise knowledge and guidance throughout my study which was provided me valuable insight in number of areas.

At the end, I am thankful to my parents, brothers, collogues who have directly or indirectly help me during this dissertation work and provided encouragement.

Ramakant I. Panchal
(10MMCC08)

Abstract

Textile machinery is one of the fastest evolving area which has an application of mechanical engineering. The modular approach towards the processing right from the stage of cotton to the fabric, allows us to observe the result of each process on its input. Cost and space being the major constraints, there is always a great scope for a mechanical engineer to apply his/her skills to improve the design.

To remain competitive in a global market place, manufacturing firm attempts to reduce the cost of the product and make the product technologically more advanced. Flyer is a component of roving machine, which is used as a part of spinning process. In the present work using the application of HyperWorks, the flyer arm has been modified which saves the material used for manufacturing the flyer.

The size optimization of the flyer is carried out with the objective of reduction in weight under the constraints of standard operating conditions. The new design of the flyer is proposed and validated using the module of HyperWorks which is equally strong but light weighted compared to the existing design.

Dynamic balancing of optimized model is carried out to align a principle inertia axis with the geometric axis of rotation. For the balanced geometry of flyer, air resistance is obtained theoretically and with Gambit and Fluent. Static analysis of the balanced geometry has been done to verify the constraint of operating condition. Comparison of weight, deflection and factor of safety has been made for different aluminium alloys.

Keywords - Flyer, Size Optimization

Contents

Declaration iii

Certificate v

Acknowledgements vi

Abstract vii

List of Figures xi

List of Tables xiii

Nomenclature xiv

Abbreviation xv

1 Introduction 1
- 1.1 Preamble . . . 1
- 1.2 Description of Flyer . . . 1
- 1.3 Problem Definition . . . 5
- 1.4 Outline . . . 5

2 Literature Survey 7

3 Finite Element Analysis of Existing Flyer 11
- 3.1 Material Properties and Operating Conditions . . . 11
  - 3.1.1 Aluminium Alloy . . . 11
  - 3.1.2 Operating Conditions . . . 11
  - 3.1.3 Structural Requirements . . . 12
- 3.2 Theoretical Analysis for Deflection of Flyer Arm . . . 12
- 3.3 Stresses In Flyer Arm (Approximate Analysis) . . . 16
- 3.4 Finite Element Analysis of the Flyer . . . 19

4 Optimization of Flyer **22**
4.1 Size Optimization . . . 23
4.1.1 Meshing of Flyer . . . 23
4.1.2 FEA Data . . . 23
4.1.3 Static Analysis . . . 24
4.1.4 Optimization . . . 24
4.2 Static Analysis of Optimized Flyer Model . . . 27
4.3 Results of Size Optimization . . . 27
4.4 FE Analysis of Optimized Model . . . 28
4.5 Deflection of Flyer Arm for Optimized Model . . . 30
4.5.1 Stresses In Flyer Arm . . . 31
4.6 Result Summary . . . 31

5 Design Modifications **33**
5.1 Introduction . . . 33
5.2 Dynamic Balancing of Flyer . . . 34
5.3 Two Plane Balancing of Flyer . . . 36
5.4 First Design Modification . . . 38
5.4.1 Result Summary for First Design Modification . . . 40
5.5 Second Design Modification . . . 40
5.5.1 Result Summary of Second Design Modification . . . 42
5.6 Third Design Modification . . . 42
5.6.1 Result Summary of Third Design Modification . . . 44
5.7 Final Modification Considering Dynamic Balancing . . . 44
5.8 Deflection of Flyer Arm for Balanced Model . . . 45
5.8.1 Stress in Flyer Arm . . . 46
5.9 Air Resistance of Proposed Geometry . . . 48
5.9.1 Theoretical Drag Force Calculation . . . 48
5.9.2 FE Analysis for Drag Force . . . 49
5.10 Design for Alternate Material . . . 51
5.10.1 Aluminium Alloy A380 . . . 52
5.10.2 Aluminium Alloy 383 . . . 54
5.10.3 Aluminium Alloy 413 . . . 55
5.10.4 Aluminium Alloy 518 . . . 56
5.10.5 Aluminium Alloy B390 . . . 57

6 Result and Discussion **59**
6.1 Deflection and Stresses for Existing model of Flyer . . . 59
6.2 Deflection and Stresses for Optimized model of Flyer . . . 61
6.3 Balancing Result . . . 62
6.3.1 FE Analysis of Optimized Balanced model of Flyer . . . 63
6.4 Drag Force & Coefficient for Proposed Geometry . . . 65
6.5 Design for Alternate Material (for optimized balanced model) . . . 65

7 Conclusion and Future Scope **67**
7.1 Conclusion 67
7.2 Future Scope 67

References **69**

List of Figures

1.1 Roving frame[3] 2
1.2 Structure of flyer 3
1.3 Flyer top [4] 4
1.4 Flyer arms [5] 4
1.5 Position of presser [6] 5

3.1 Simplified model of non-presser arm and loads on the non-presser arm 13
3.2 Loads on the first section 14
3.3 Loads on the second section 15
3.4 Section of flyer arm 16
3.5 Solid model of flyer 19
3.6 Total deformation of flyer 20
3.7 von-Mises stress on flyer 20

4.1 Mesh model of flyer 24
4.2 Displacement plot before size optimization 25
4.3 Thickness plot after size optimization 26
4.4 Displacement plot after size optimization 27
4.5 Redesign of flyer 28
4.6 Total deformation of redesign flyer 29
4.7 von-Mises stress of redesign flyer 29

5.1 Top view of flyer assembly 35
5.2 Distance of unbalance mass from the origin 35
5.3 Total deformation in first modified design of flyer 39
5.4 von-Mises stress on first modified design of flyer 39
5.5 Total deformation in second modified design of flyer 41
5.6 von-Mises stress on second modified design of flyer 41
5.7 Total deformation in third modified design of flyer 43
5.8 von-Mises stress on third modified design of flyer 43
5.9 Redesign of flyer 44
5.10 solid model of proposed geometry 49
5.11 Mesh model of proposed geometry 50
5.12 Drag co-efficient 50

5.13 Total deformation for aluminium alloy A380 53
5.14 von-Mises Stress for aluminium alloy A380 53
5.15 Total deformation for aluminium alloy 383 54
5.16 von-Mises stress for aluminium alloy 383 54
5.17 Total deformation for aluminium alloy 413 55
5.18 von-Mises stress for aluminium alloy 413 55
5.19 Total deformation for aluminium alloy 518 56
5.20 von-Mises stress for aluminium alloy 518 56
5.21 Total deformation for aluminium alloy B390 57
5.22 von-Mises stress for aluminium alloy B390 57

6.1 Total deformation of existing flyer 60
6.2 von-Mises stress on existing flyer 60
6.3 Total deformation of optimized model of flyer 61
6.4 von-Mises stress on optimized model of flyer 62
6.5 Total deformation of optimized balanced model of flyer 64
6.6 Von-Mises Stress on optimized balanced model of flyer 64
6.7 Comparison for alternate material 66

List of Tables

3.1 Different parameters for each segment 17
3.2 Factor of safety calculation for different segments 18

4.1 Various segment wise allocation of thickness 25
4.2 Different segment thickness obtain after the size optimization 26
4.3 Different parameters for each segment 31
4.4 Factor of safety calculation for different segments 32

5.1 Location of mass at each quadrant 36
5.2 Horizontal and vertical component of couple 38
5.3 Horizontal and vertical component of force 38
5.4 Different parameters for each segment 46
5.5 Factor of safety calculation for different segments 47
5.6 Mechanical properties of aluminum alloy[21] 51
5.7 Chemical composition of aluminum alloy[21] 52
5.8 Result of analysis of flyer for different material 58

6.1 Deflection at free end of flyer 60
6.2 Deflection at free end of flyer 61
6.3 Deflection at free end of flyer 63
6.4 Result comparison of existing and optimized balanced model 63
6.5 Drag force for proposed geometry 65

Nomenclatures

A_1 ..... Area of cross-section of the first section
A_2 ..... Area of cross-section of the second section
C_i ..... Integral constants, i=1,2,3,4
E ..... Modulus of Elasticity
I_1 ..... Moment of Inertia over the first section
I_2 ..... Moment of Inertia over the second section
L_1 ..... Length of first section
L_2 ..... Length of second section
b_1 ..... Width of cross-section of flyer
h_1 ..... Depth of cross-section of flyer
b_2 ..... Width of cross-section of flyer
h_2 ..... Depth of cross-section of flyer
M_a ..... Moment at x=0
M_x ..... Moment at x=x
μ ..... Poison's ratio
q_1 ..... Load intensity at the first section
q_2 ..... Load intensity at the second section
y_1 ..... Deflection at first section
y_2 ..... Deflection at first section and second section
V_a ..... Load at x=0
V_x ..... Load at x=x
ρ_{Al} ..... Density of aluminium
ω ..... Angular velocity of the flyer about y-axis
σ_b ..... Bending Stress
ΣM_b ..... Total bending moment
A ..... Reference area
C_d ..... Drag coefficient
F ..... Drag force
V ..... Velocity
ρ ..... Density of fluid

Abbreviation

FOS ..... Factor of Safety
CAE ..... Computer Aided Engineering
DOF ..... Degree of Freedom
FEA ..... Finite Element Analysis
SEG ..... Segment

Chapter 1

Introduction

1.1 Preamble

Textile manufacturing is a process of converting different types of fibers into yarn, then fabric and in turn textile. During the process of converting fibers in to yarn, the roving which is a long and narrow bundle of cotton fibers needed to be spin to insert twist within it. To remain competitive in a global market place, manufacturing firm attempt to reduce the cost of the product and make the product technologically more advanced. In this project work modified design for the flyer with reduction in weight is obtained, while the total deflection and von-Mises stresses are within the limit.

1.2 Description of Flyer

Flyer is a component of roving machine, which is used as a part of spinning process.[1] Since the strands are parallelized, they are not strong enough and this can lead to breakage. The reason for breakage could be the tension in the strands, its own weight and air currents at high speed of operations. After drafting the strands are passed through flyers to introduce a roving twist into the strands. The roving frame is shown in Figure 1.1 the strand from the drafting arrangement enters the top of flyer and bobbin winding will take place.[2]

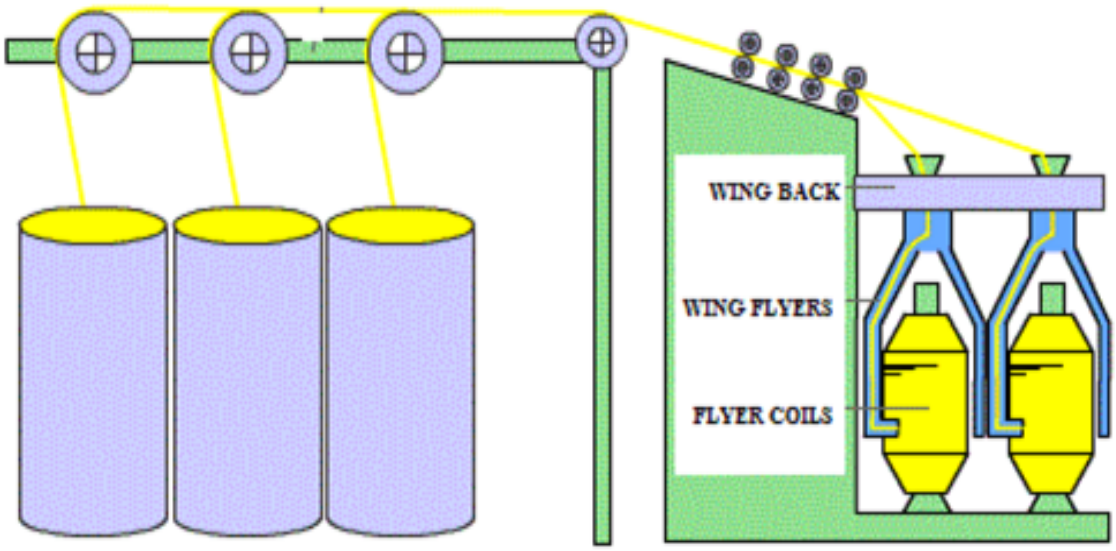

Figure 1.1: Roving frame[3]

Flyers have been made in various forms but the only commercial flyer of today is the inverted "U" that fits on the top of the spindle and revolves with it. The structure of the flyer is shown in Figure 1.2.

Flyer consist of following parts.

- Spindle shaft
- Flyer Top
- Hollow arm
- Solid arm
- Presser

Figure 1.2: Structure of flyer
(Courtesy : Inspiron Engg. Pvt. Ltd.)

The strand passes through the flyer top without wrapping, the shape of the flyer top is shown in Figure 1.3. Since the flyer is rotating at 1200rpm, so the strand must be protected against strong air currents. For this purpose, one of the flyer arm is hollow and the strand is drawn through the guide tube fully protected it against the air flows. The second full arm serves to balance the groove arm. Various design of flyer arm is shown in Figure 1.4, the slot in the flyer arm is usually made straight as shown in Figure 1.4(A), but for high speed and fine ravings there is an advantage in making winding with slot in the flyer arm as shown in Figure 1.4(B). This prevents the centrifugal force sending the roving through the slot.[4]

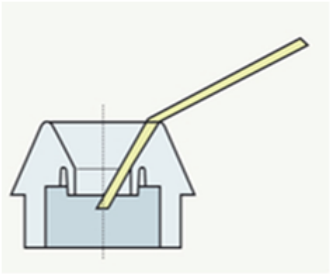

Figure 1.3: Flyer top [4]

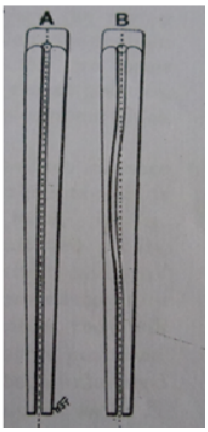

Figure 1.4: Flyer arms [5]

The presser is composed of two parts:

(1) Paddle or presser, to roving on the bobbin.

(2) Presser rod, running up the side of leg.

The presser arm is shown in Figure 1.5. The strand from the drafting arrangement enters the top of the hollow arm travels downward and emerges at the bottom where it is wound around a presser finger and take-up package. Presser-finger bar is swiveling on the side of the arm, presser-finger arm working round the leg as a center. Weight of the presser-finger bar is greater than presser-finger arm, when it revolves from the center of the spindle it has greater tendency to fly away from the center. The

centrifugal force tending to move the presser-finger rod outwards being resisted by the bobbin, which prevents the other end of the paddle moving inwards.[4]

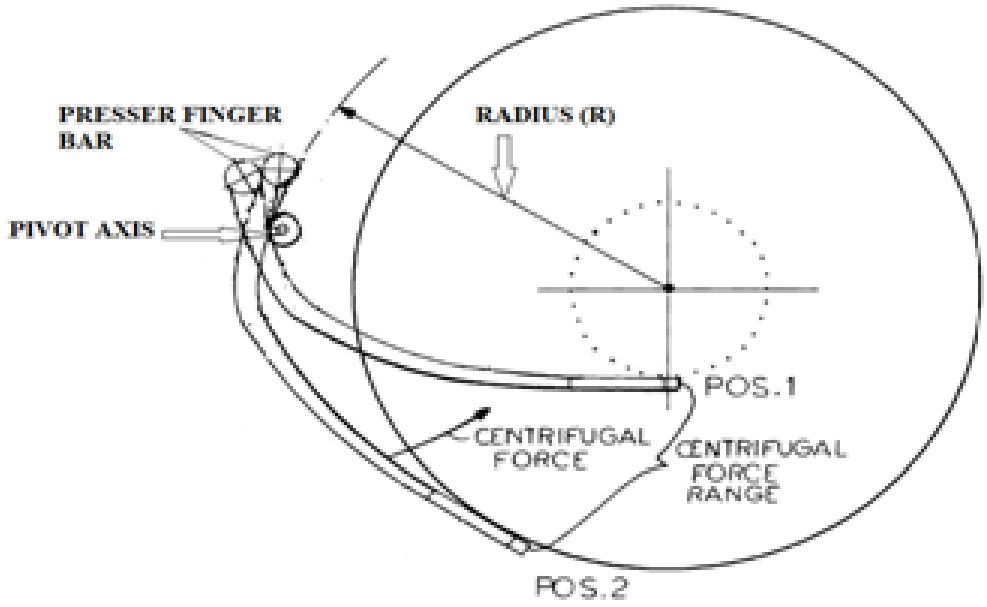

Figure 1.5: Position of presser [6]

1.3 Problem Definition

The basic objective is to modified design of flyer, with saving in raw materials and then analyze it using finite element analysis software to verify the new design of flyer for strength and withstand the constraints of the operating conditions.

1.4 Outline

The first chapter describes the introduction and problem definition. The second chapter on the literature survey deals with various contribution, patent of flyer and

optimization technics explained. Theoretical and finite element analysis of the existing flyer arm is explained in third chapter. The fourth chapter describes the size optimization of flyer with the objective of reduction weight using the Altair OPTISTRUCT tool and also the modification in geometry of the flyer according to the result of size optimization is explain in the same chapter. The fifth chapter describes the dynamic balancing of flyer, aerodynamic air resistance of flyer and design for alternate material. There is discussion on results in sixth chapter. And finally conclusion and future scope of work has been discussed in seventh chapter.

Chapter 2

Literature Survey

The textile manufacturing process is a very exhaustive process which takes place in a number of machines. The manufacturing process involves a lot of transportation and handling of the in-feed to various machines and output of those machines emphasis need to be placed on the fact that the quantity of the package does not deteriorate during this process. At text book level various manufacturing process like preparation of bales, spinning, weaving, knitting and wet processing are explained in detail.[1],[2],[3],[4],[5]

Frederic Jean, et.al[6] designed the body of flyer provides two identical limbs and is formed as a single hollow piece and in that the roving guide is constituted by a tube inside the limb and extending on one hand the upper part of the hollow shaft and other hand into the corresponding arm. To improve the output of roving frame and attaining greater rotational speed the flyer body and legs formed with aerodynamic profiles.

Peter Novak, et. al[7] has designed flyer for high rotational speeds. According to the invention the flyer arms at their free ends are connected rigidly with a horizontal ring. Straight guide tube is supported between upper and lower pivoting bearing, and it rotates about its longitudinal axis. Guide tube can be made any suitable desired material, e.g. Also partially from a ceramic material.

Background of the invention done from British patent number 380745 in which two

flyer arms are formed by steel tubes and which is provided with two additionally auxiliary arms The lower ends are connected by a horizontal ring for strength to achieve high rotational speeds. In this flyer no presser finger is provided and thus the deposition of the roving onto the bobbin tube is uncontrolled. Another invention done from German patent number 1685910 in which flyer arm guiding the roving, for that steel tube is provided which is surrounded by aluminum. Special presser finger is provided for guiding roving. In this flyer absent of horizontal ring so distance of the lower ends of flyer arm increases at high rotational speed of flyer which increase flyer breakage.

Wegger Hans-Peter, et. al[8] designed a flyer for a roving frame which has a pressing finger swingably mounted with its pressing-finger rod and pressing-finger arm on one arm of the flyer, the pivot axis lying in the center of the connection of the pressing finger with the flyer arm. This flyer arm is rotates about the center of the bobbin so that the pivot axis describes a predetermined radius "r" as the flyer arm orbits the bobbin. The pressing finger rod is acted upon by an actuating element transverse to the pivot axis to swing the pressing-finger arm into an outwardly swung position. The objective of invention is wide opening of the pressing finger, enabled for bobbin change and the pressing finger can automatically be guided against the empty core sleeve for automatic spinning start-up without continuous loading the pressing finger by a pressing force against the sleeve or bobbin. Background of the invention done from German patent number 19543716 describes flyers for roving frames which have pressing fingers comprised of pressing-finger rods or bars and pressing-finger arms carrying pressing-finger plates. The pressing-finger rod which lies outside a pivot axis can be swung by an actuating element effective transverse to the pivot axis so that the pressing finger can be pivoted into an outwardly swung position and can be held in this position. The pressing finger can be swung outwardly sufficiently that the full bobbin can be removed from the rotation region on the flyer.

At text book level theoretical analysis to obtain deflection of the variable cross-section are explained in detail.[9],[10],[11]

Optimization is the process of finding the functions which gives the minimum or maximum value of the function. There are mainly three types of optimization topology, shape, and size.

In topology optimization the optimal structure shape with appropriate geometry is issued as a design proposal.[12] Therefore an idea (2D and 3D) with a homogenous material is used. Subsequently the functionally boundary conditions are applied.

Size optimization, involves modifications of cross-section or thickness distribution throughout the structure of finite element.[12],[13]

Patel Nilesh et. al[13] has done Optimal design of Tilt Beam for reduced deflection and weight compared to existing conventional design,Topology optimization was carried out with compliance as constraint and volume fraction as an objective. The optimal thickness of all structural members is decided by size optimization.

In shape optimization,t he outer boundary of structure is modified to solve the optimization problem.[14],[15] Using finite element models, the shape is defined by the grid point locations. Hence the shape modifications change this location. In order to avoid to mesh distortion due to shape changes, changes of the shape of the structural boundary must be translated into changes of the interior of the mesh.

Vibration caused by mass unbalance is common in rotating machinery. Rotating components need to be balance to ensure smooth running when in operation. The mass unbalance in a rotating system often produces excessive synchronous force that reduces the life of various mechanical elements. Therefore balancing is important in manufacturing and maintenance process of rotating machines. For balancing of rotating components balancing grades are referred from standard.[16] At text book level different balancing technique like static balance and dynamic balance are explained in detail.[17],[18]

It is known that any surface in contact with a flowing fluid is subject to a force exerted by the fluid. This force is commonly called a drag force. The drag coefficient is a well known parameter used to characterize the drag force a body immersed in a fluid experiences due to relative motion between the body and the fluid.[19],[20]

As flyer are made from die casting process, different aluminium alloys are chosen for improvement in the performance required. For various aluminium alloys properties are obtained from various standard.[21]

Chapter 3

Finite Element Analysis of Existing Flyer

In this chapter theoretical and finite element analysis of the existing flyer arm is presented. As the major area of concern is to reduce the weight of the flyer arm has been taken into the consideration for analysis. The flyer arm has been evaluated for inertia load, as it rotates at 1200rpm. Using the proper boundary conditions static deflection and stresses were obtained with theoretical and finite element analysis.

3.1 Material Properties and Operating Conditions

3.1.1 Aluminium Alloy

Density=2700 kg/m^3

Modulus of elasticity(E) = 7.1GPa

Poisson's ratio= 0.3

3.1.2 Operating Conditions

Running speed = 1200rpm

3.1.3 Structural Requirements

Allowable expansion of arms, during rotation $\leq 5mm$

3.2 Theoretical Analysis for Deflection of Flyer Arm

In this section, stress and the deflection of the non-presser arm is obtained. The arm is modeled as a variable cross-section cantilever beam.[9],[10] Simplified model of non-presser arm and loads on the non-presser arm is shown in Figure 3.1. following parameters are consider for the analysis.

Parameter:

ρ_{Al}=2700 kg/m^3 ; R=0.09 m ; ω=125.6 rad/s

$b_1 = 0.043$ m ; $h_1 = 0.047$ m ; $L_1 = 0.112$ m

$b_2 = 0.025$ m ; $h_2 = 0.042$ m ; $L_2 = 0.277$ m

E=7.1 GPa ; $I_1 = 5.468e^{-8}m^4$; $I_2 = 3.3e^{-8}m^4$

$$A_1 = (b_1 h_1) \times \left\{1 - \frac{0.419x}{L_1}\right\} \times \left\{1 - \frac{0.106x}{L_1}\right\} \tag{3.1}$$

$$A_2 = (b_2 h_2) \times \left\{1 - \frac{-0.18(x - L_1)}{L_2}\right\} \times \left\{1 - \frac{0.2(x - L_1)}{L_2}\right\} \tag{3.2}$$

$$q_1 = \rho_{Al} A_1 \omega^2 r \tag{3.3}$$

$$q_1 = 5500.94\ N/m$$

$$q_2 = \rho_{Al} A_2 \omega^2 r \tag{3.4}$$

$$q_2 = 3795.07\ N/m$$

$$V_A = q_1\ L_1 + q_2\ L_2 \tag{3.5}$$

$$V_A = 1667.34\ N/m$$

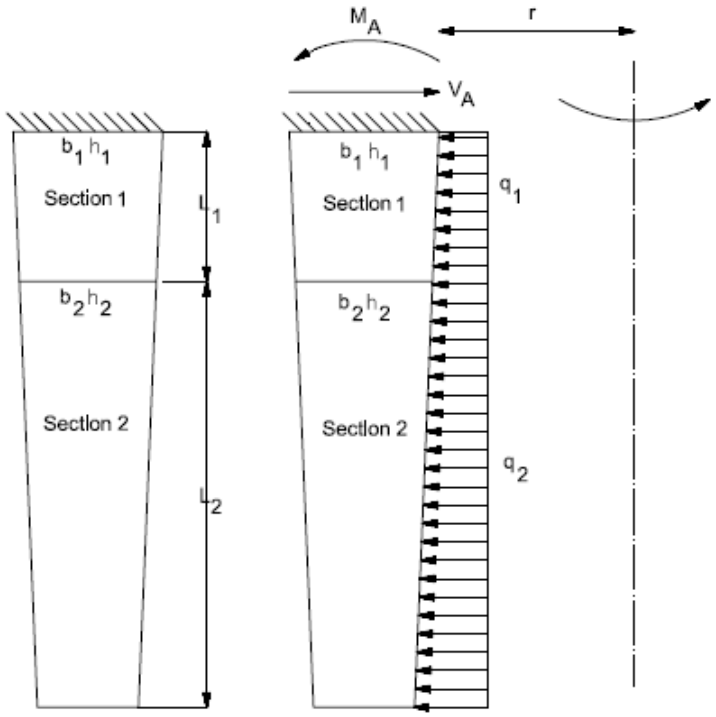

Figure 3.1: Simplified model of non-presser arm and loads on the non-presser arm

$$M_A = \ q_1 L_1 \frac{L_1}{2} + q_2 L_2 (L_1 + \frac{L_2}{2}) \tag{3.6}$$

$$M_{A=}\ 297.83 N/m$$

for 0 < x < L_1(refer Figure 3.2)

$$V_A + V_X = \ q_1 \ x \tag{3.7}$$

$$M_x = \ -q_1 x \ \frac{x}{2} - M_A + V_A \times x \tag{3.8}$$

$$M_x = EI_1 \frac{d^2 y_1}{dx^2}$$

$$EI_1 \frac{d^2 y_1}{dx^2} = \ -q_1 \frac{x^2}{2} - M_A + (q_1 L_1 + q_2 L_2)\, x \tag{3.9}$$

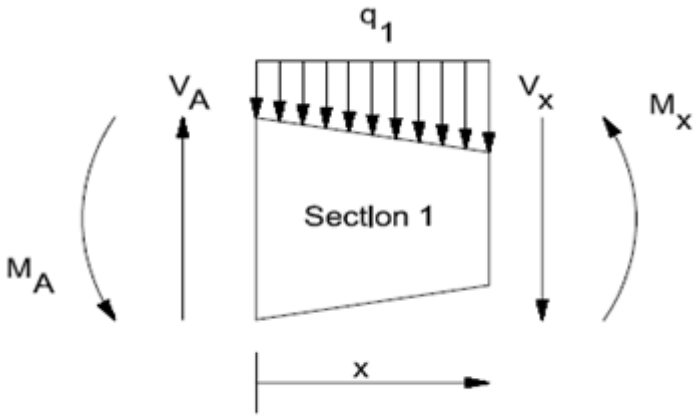

Figure 3.2: Loads on the first section

Further integration

$$EI_1\frac{dy_1}{dx} = -q_1\frac{x^3}{6} - M_A x + (q_1L_1 + q_2L_2)\frac{x^2}{2} + c_1 \tag{3.10}$$

Upon further integration

$$EI_1y_1 = -q_1\frac{x^4}{24} - M_A\frac{x^2}{2} + (q_1L_1 + q_2L_2)\frac{x^3}{6} + c_1x + c_2 \tag{3.11}$$

for $L_1 < \mathrm{x} < L_1 + L_2$ (refer Figure 3.3)

$$M_x = -q_2\frac{(x-L_1)^2}{2} - q_1L_1\left(x - \frac{L_1}{2}\right) - M_A + V_A \times x \tag{3.12}$$

$$M_x = EI_2\frac{d^2y_2}{dx^2}$$

$$EI_2\frac{d^2y_2}{dx^2} = -q_2\frac{(x-L_1)^2}{2} - q_1L_1\left(x - \frac{L_1}{2}\right) - M_A + (q_1L_1 + q_2L_2)\,x \tag{3.13}$$

$$EI_2\frac{dy_2}{dx} = -q_2\frac{(x-L_1)^3}{6} - q_1\frac{L_1}{2}(x - \frac{L_1}{2})^2 - M_Ax + (q_1L_1 + q_2L_2)\frac{x^2}{2} + c_3 \tag{3.14}$$

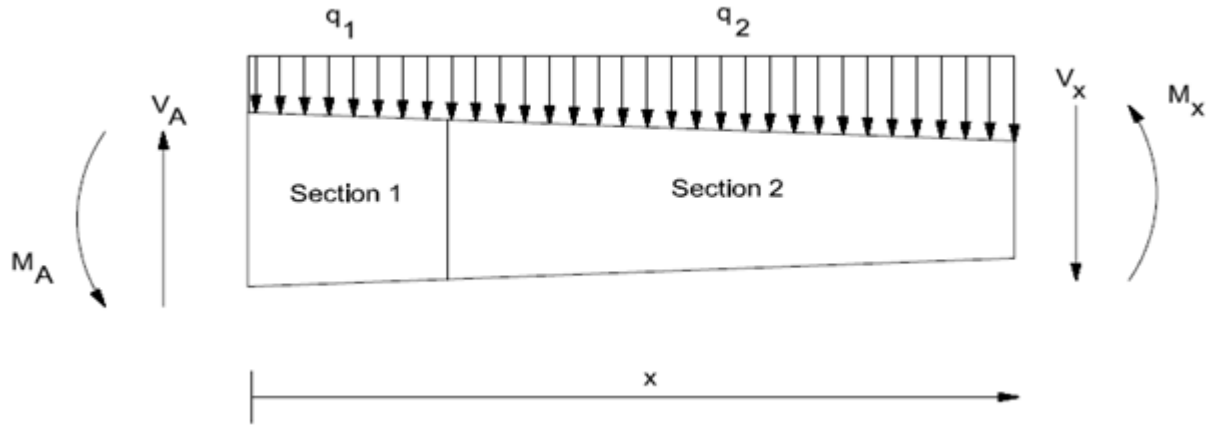

Figure 3.3: Loads on the second section

$$EI_2y_2 = -q_2\frac{(x-L_1)^4}{24} - q_1\frac{L_1}{6}(x-\frac{L_1}{2})^3 - M_A\frac{x^2}{2} + (q_1L_1 + q_2L_2)\frac{x^3}{6} + c_3x + c_4 \quad (3.15)$$

boundary conditions,

$$x = 0, \qquad y_1 = 0 \quad (3.16)$$

$$x = 0, \qquad \frac{dy_1}{dx} = 0 \quad (3.17)$$

$$x = l_1, \qquad y_1 = y_2 \quad (3.18)$$

$$x = l_1, \qquad \frac{dy_1}{dx} = \frac{dy_2}{dx} \quad (3.19)$$

Now with given boundary conditions,

Solving the equation (3.10) and(3.17) gives $C_1 = 0$

Solving the equation (3.11) and (3.16) gives C_2=0

Solving the equation (3.10), equation (3.14), and equation (3.19)

Get the Value of $C_3 = 7.8107$

Solving the equation (3.11), equation(3.15), and equation (3.18)

Get the Value of C_4= -0.3618

Substitute all these values in equation (3.15)

Get the Value of y_2 = -0.0019 m

So the deflection of non-presser arm by this method = 1.9 mm.

3.3 Stresses In Flyer Arm (Approximate Analysis)

The arm of the flyer is divided into five segment as shown in Figure 3.4. For various section bending moment and section modulus are calculated. Finally Bending stress and factor of safety for each section calculated. Refer Table 3.1 and 3.2 for factor of safety calculation at each section.

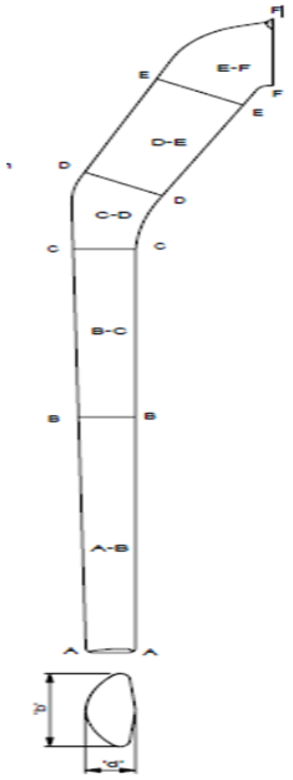

Figure 3.4: Section of flyer arm

Following parameters are consider for calculate the value of factor of safety at each section.

Parameter:

N = 1200rpm

Proof stress of aluminum alloy: 175 N/mm^2

Measure and calculate parameters for each segment are tabulated below.

Table 3.1: Different parameters for each segment

Segment	Vol. 10^4 mm^4	Mass (kg)	Radius (mm)	C. force (kg)	M.I. 10^4 (mm^4)	Distance (Y) mm	Length of C.G.of segment from sections (mm)				
							Sec. B	Sec. C	Sec. D	Sec. E	Sec. F
A-B	12.6	0.34	88.44	48.50	2.430	10.7	82.4	193.2	226.5	289.2	305.2
B-C	8.650	0.23	89.73	33.76	2.97	11.84	-	55.2	88.54	151.2	167.2
C-D	3.985	0.11	90.207	15.52	11.21	21.05		-	11.3	74.0	90.0
D-E	8.880	0.24	70.56	27.31	18.6	21.39			-	22.17	38.17
E-F	6.971	0.19	46.46	14.05	24.8	20.10				-	13.06

The Table 3.2 shows that value of factor of safety is higher in each segment, hence there is scope for reduction in weight, available by modifying the design of the flyer.

Table 3.2: Factor of safety calculation for different segments

	Section B			Section C			Section D			Section E			Section F		
Segment	Centfugal-force (N)	Length (mm)	Bending moment	Centfugal-force (N)	Length (mm)	Bending moment	Centfugal-force (N)	Length (mm)	Bending moment	Centfugal-force (N)	Length (mm)	Bending moment	Centfugal-force (N)	Length (mm)	Bending moment
A-B	475.85	82.4	39210.04	475.85	193.2	91934.22	475.85	226.5	107780.03	475.85	289.2	137615.82	475.85	305.2	145229.42
B-C				331.18	55.2	18281.136	331.18	88.54	29322.677	331.18	151.2	50074.416	331.18	167.2	55373.296
C-D							152.25	11.3	1720.425	152.25	74	11266.5	152.25	90	13702.5
D-E										267.911	22.17	5939.5869	267.911	38.17	10226.163
E-F													137.83	13.06	1800.0598
Σ MB	Total Bending Moment @ Sec. B		39210.04	Total Bending Moment @ Sec.C		110215.36	Total Bending Moment @ Sec. D		138823.13	Total Bending Moment @ Sec. E		204896.32	Total Bending Moment @ Sec. E		226331.44
W_{xu}	Moment of resistance (I/Y)		2256			2510			5750			8700			12340
σ_b	Total Bending Stress @ Sec. B		17.380337	Total Bending Stress @ Sec. C		43.9105	Total Bending Stress @ Sec. D		24.143153	Total Bending Stress @ Sec.E		23.551301	Total Bending Stress @ Sec. F		18.341284
	FOS		10.0688497			3.98537932			7.24843202			7.43058723			9.54131698

3.4 Finite Element Analysis of the Flyer

The solid model of flyer as shown in Figure 3.5 is prepare in pro/e and meshed. The static structural analysis has been carried out with rotational angular velocity of 125.6 rad/s and the spindle shaft is in contact with the flyer was constrained for all DOF. The solution has been obtained for total displacement and von-Mises stress distribution within model. Deflection and the von-Mises stress plot for flyer arm are shown in Figure 3.6 and Figure 3.7 respectively.

Figure 3.5: Solid model of flyer

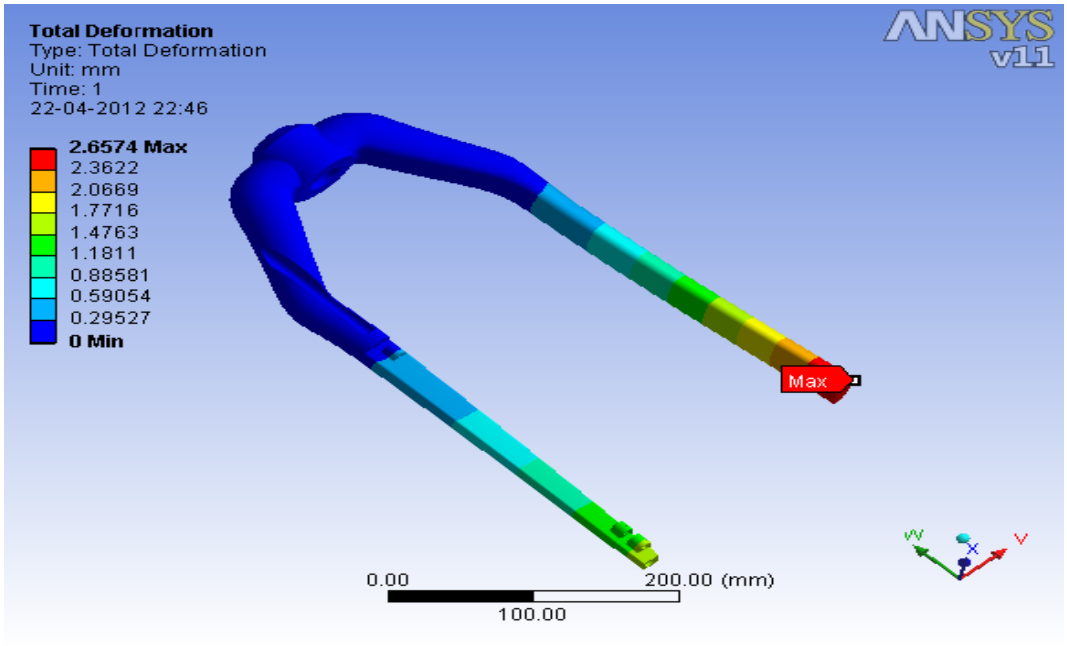

Figure 3.6: Total deformation of flyer

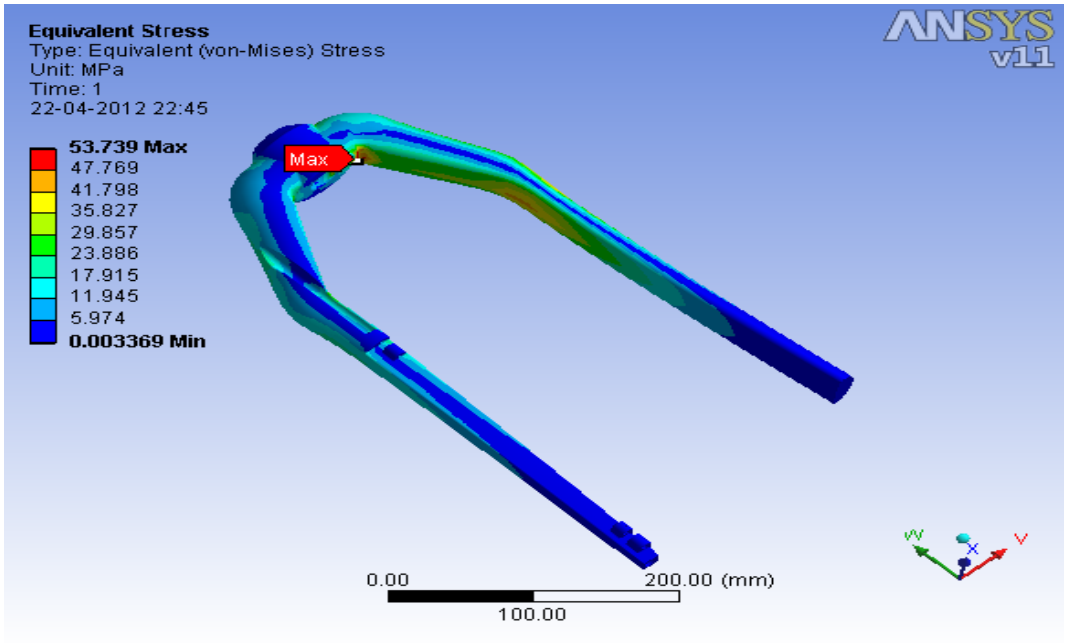

Figure 3.7: von-Mises stress on flyer

The FE analysis shows the location of the maximum von-Mises stresses near the junction of the arm and the shaft locating hub, as the geometry is constrained near the hub portion. The free end of the flyer arm deflects maximum as that end being the free end.

Chapter 4

Optimization of Flyer

In this chapter optimization of flyer is presented. The design modification of the flyer involves change in shape of the flyer in order to reduce the raw material. While carrying out modification, total deflection and equivalent stresses are to be kept within the range. The concept of redesigning the flyer can be evaluated using the optimization tool called Altair OPTISTRUCT. This CAE tool has capability for conducting topology optimization, shape optimization, size optimization etc.

Topology optimization is used to find out the optimal structure shape with appropriate geometry is issued as a design proposal. Therefore an idea (2D and 3D) with a homogenous material is used. Subsequently the functionally boundary conditions are applied. In size optimization, the properties of structural elements such as shell thickness, beam cross-sectional properties, spring stiffness, and mass are modified to solve the optimization problem. [12],[13],[14] Shape optimization is process to change the shape of the structure. This may include finding the optimum shape to reduce stress concentrations to changing the cross-sections to meet specific design requirements. Therefore, to define the shape modifications and the nodal movements to reflect the shape changes.[15]

4.1 Size Optimization

Size optimization is process of changing the shape of structure without adding or removing additional features. It involves the changing the dimensional properties of either 1-d or 2-d elements. These properties include area, moments of inertia of the 1-d elements, and the thickness of 2-d elements. Size optimization is an FE based optimization technique in which the object design is optimized by varying the thickness distribution throughout the structure. Prior to size optimization it is necessary to provide a geometric model reduced to surface or line segments. For the case of flyer the mid surface has been extracted and is divided into 14 different segments for assigning various thicknesses.

4.1.1 Meshing of Flyer

The mesh used for size optimization is a shell element mesh. These elements are in OPTISTRUCT called CQUAD4. Quadrilateral elements are elements with 2 sides and 4 nodes. Figure 4.1 shows the mesh model of the flyer. In order to make the structural behavior same as that of original model, the material is taken homogenous, isotropic, linear and temperature independent. Material properties of aluminium is applied to the model as shown below.

Density=2700 kg/m^3
Modulus of elasticity(E) = 7.1GPa
Poisson's ratio= 0.3

4.1.2 FEA Data

Element type:- CQUARD
No. of elements:- 13360
No. of nodes:- 14095

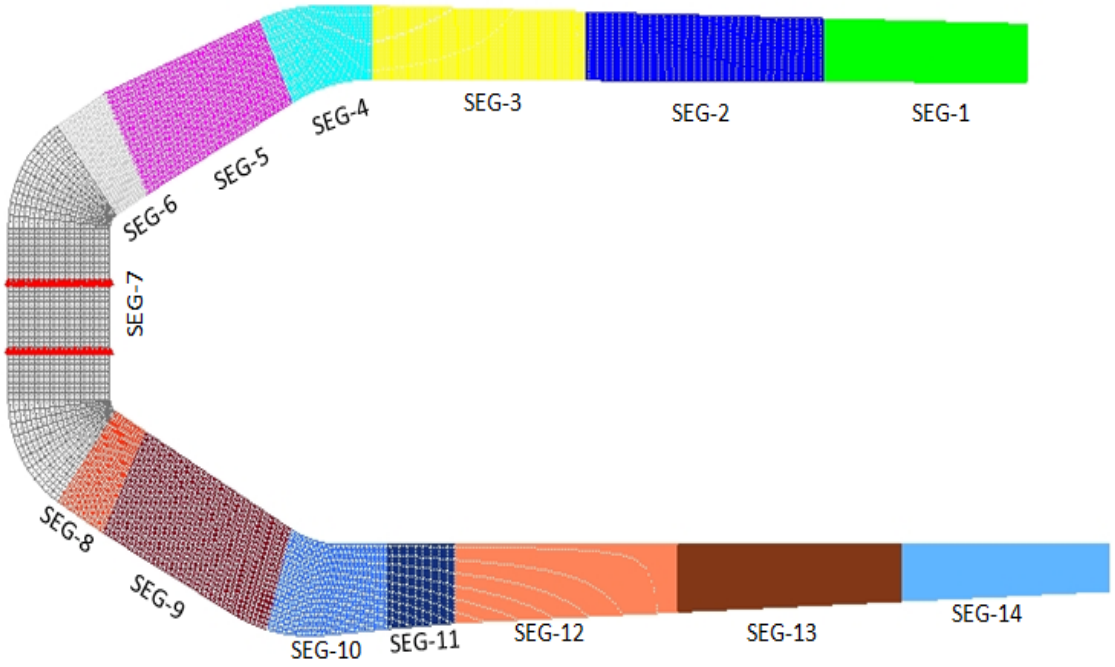

Figure 4.1: Mesh model of flyer

4.1.3 Static Analysis

After defining the material property, boundary conditions and loading conditions has been applied to carry out static analysis. The deformation of flyer arm is obtained as 2.64 mm as shown in Figure 4.2.

4.1.4 Optimization

The following are the details of optimization.

Objective:- To reduce the weight of the segment.

Design variable:- Thickness of the segment.

Design Constraint:- Displacement.

Various segment wise allocation of thickness for the 2D meshed model of flyer arm are as shown in Table 4.1. The optimized thickness after design iterations for various segments is shown in Figure 4.3 and values are given in Table 4.2.

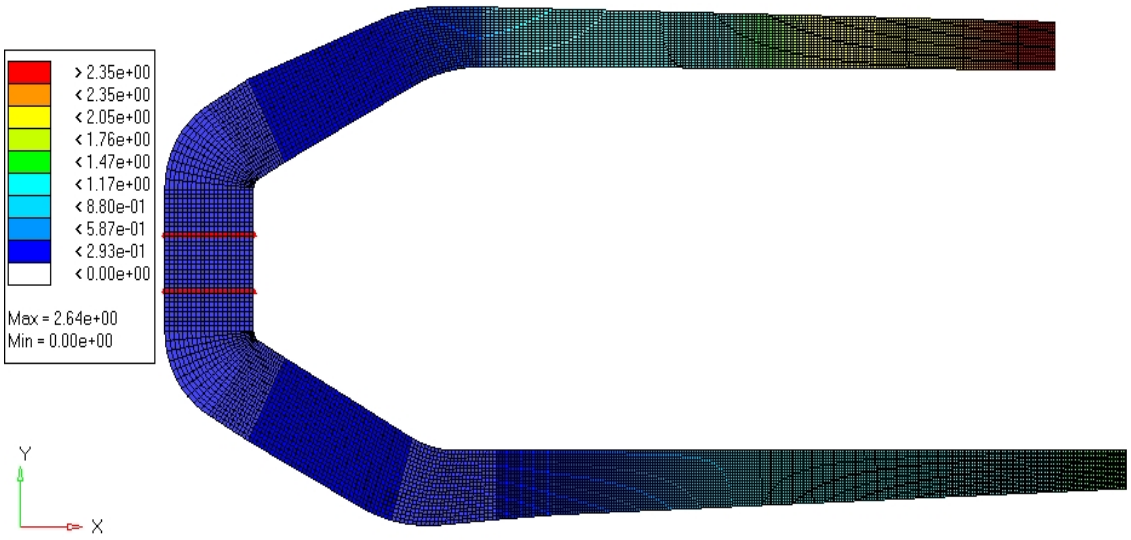

Figure 4.2: Displacement plot before size optimization

Table 4.1: Various segment wise allocation of thickness

	Label	Lower Bound	Design Variable	Upper Bound
1	THCK1	5.000E+00	4.950E+01	5.950E+01
2	THCK2	1.000E+01	4.725E+01	5.725E+01
3	THCK3	1.500E+01	4.425E+01	5.425E+01
4	THCK4	2.000E+01	4.200E+01	5.200E+01
5	THCK5	2.300E+01	4.100E+01	5.100E+01
6	THCK6	2.700E+01	4.500E+01	5.500E+01
7	THCK7	2.900E+01	4.700E+01	5.700E+01
8	THCK8	2.700E+01	4.500E+01	5.500E+01
9	THCK9	2.300E+01	4.100E+01	5.100E+01
10	THCK10	1.800E+01	3.600E+01	4.600E+01
11	THCK11	1.500E+01	2.800E+01	3.800E+01
12	THCK12	1.366E+01	2.400E+01	3.800E+01
13	THCK13	1.233E+01	2.000E+01	3.000E+01
14	THCK14	1.100E+01	1.600E+01	2.600E+01

Table 4.2: Different segment thickness obtain after the size optimization

USER-ID	PROP-TYPE	PROP-ID	ITEM-CODE	PROP-VALUE
1	PSHELL	15	T	6.000E+00
2	PSHELL	16	T	1.100E+01
3	PSHELL	17	T	1.600E+01
4	PSHELL	18	T	2.100E+01
5	PSHELL	19	T	2.400E+01
6	PSHELL	20	T	2.800E+01
7	PSHELL	21	T	3.000E+01
8	PSHELL	22	T	2.800E+01
9	PSHELL	23	T	2.400E+01
10	PSHELL	24	T	1.900E+01
11	PSHELL	25	T	1.600E+01
12	PSHELL	26	T	1.466E+01
13	PSHELL	27	T	1.333E+01
14	PSHELL	28	T	1.200E+01

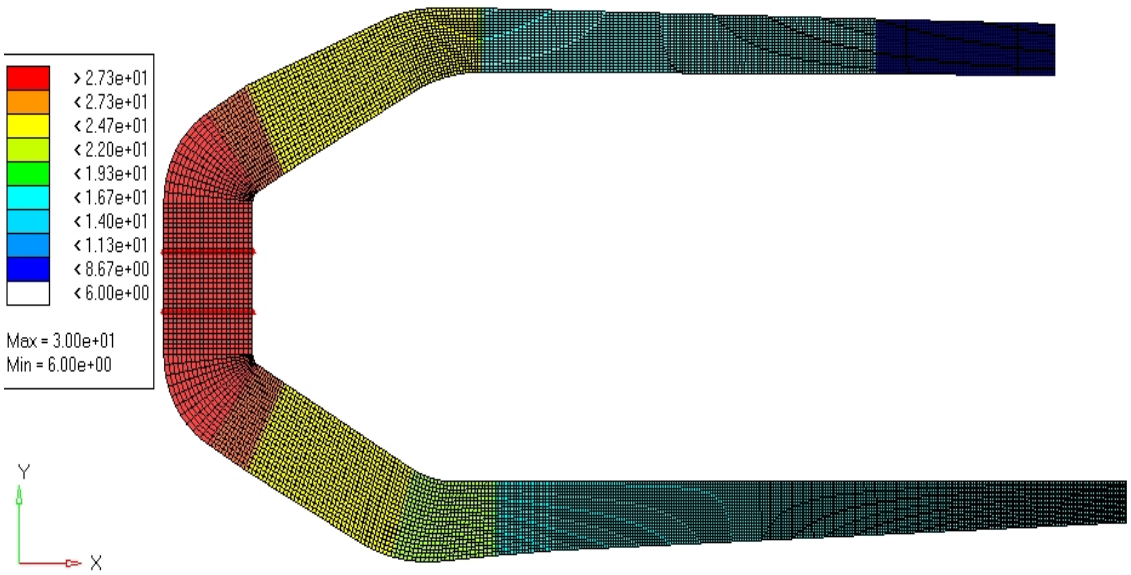

Figure 4.3: Thickness plot after size optimization

4.2 Static Analysis of Optimized Flyer Model

For the optimized model the same boundary conditions, loading conditions has been applied to surface model with the thickness of different segments obtained from size optimization. The deformation profile obtained from the static analysis is as shown in Figure 4.4. The maximum deformation obtained is 1.60 mm which is less than the deformation with the original profile.

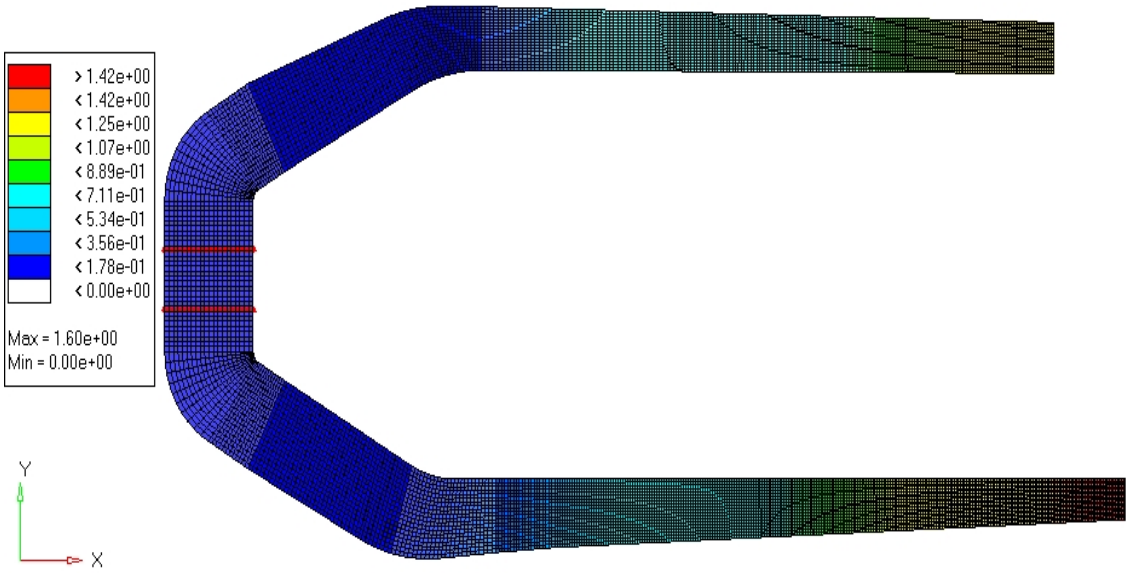

Figure 4.4: Displacement plot after size optimization

4.3 Results of Size Optimization

From the optimized result for thickness at various segment, modified 3D solid model of flyer is prepared in pro/e. as shown in Figure 4.5.

Figure 4.5: Redesign of flyer

4.4 FE Analysis of Optimized Model

For the optimized model considering the same boundary conditions, loading conditions of existing flyer, the static structral analysis has been done the plot for deflection and maximum von-Mises stress plots are obtained as shown in Figure 4.6 and 4.7 respectively.

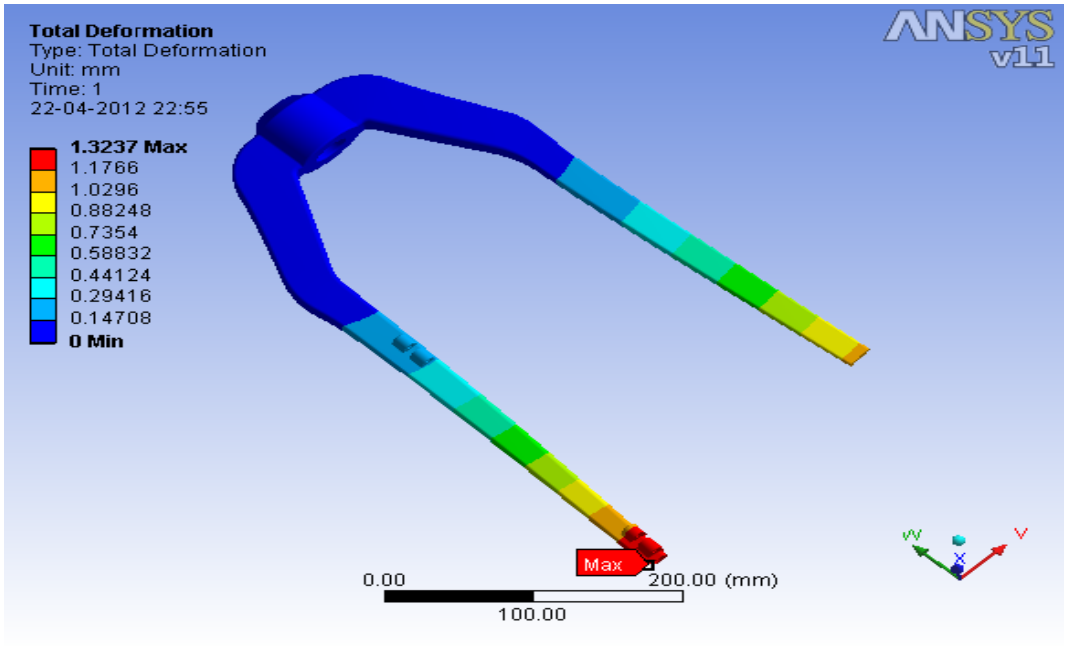

Figure 4.6: Total deformation of redesign flyer

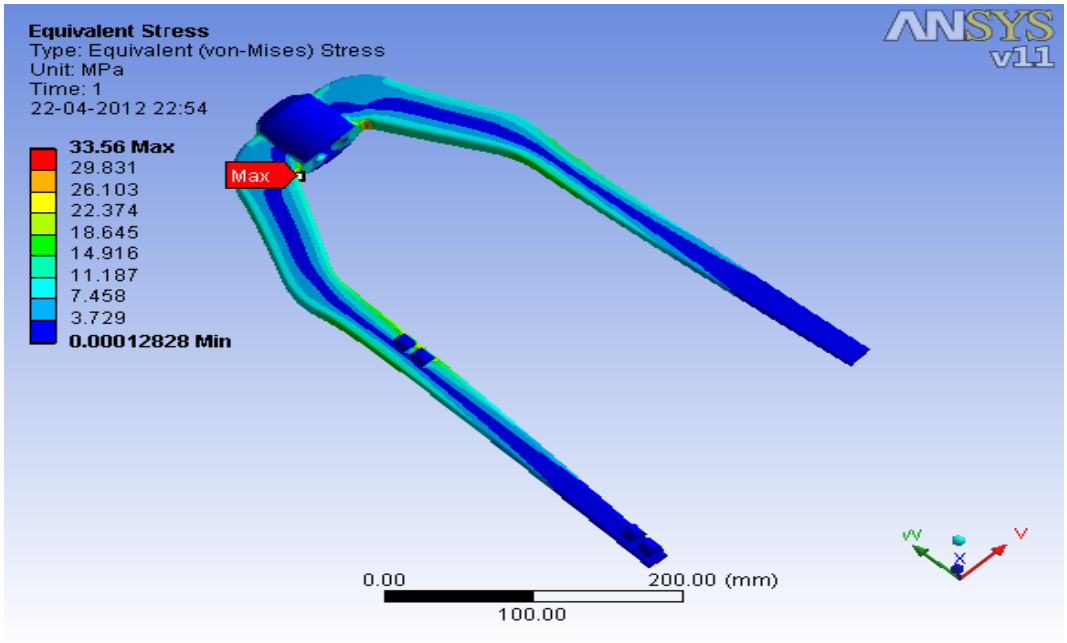

Figure 4.7: von-Mises stress of redesign flyer

The FE analysis shows the location of the maximum von Mises stresses near the junction of the arm and the shaft locating hub, as the geometry is constrained near the hub portion. The free end of the flyer arm deflects maximum as that end being the free end.

4.5 Deflection of Flyer Arm for Optimized Model

From the basic of solid mechanics, as explained in section 3.2 and 3.3 deflection at the end of flyer arm and stresses at various segment are obtained as shown in Figure 3.5. and table 4.3 and table 4.4 respectively. Following parameters are consider to calculate the value of deflection.

Parameter

ρ_{Al}=2700 kg/m^3 ; R=0.09 m ; ω=125.6 rad/s

$b_1 = 0.043$ m ; $h_1 = 0.03$ m ; $L_1 = 0.112$ m

$b_2 = 0.025$ m ; $h_2 = 0.021$ m ; $L_2 = 0.277$ m

E=7.1 GPA ; $I_1 = 2.7285e^{-8}m^4$; $I_2 = 3.999e^{-9}m^4$

$$A_1 = (b_1 h_1) \times \left\{1 - \frac{0.419x}{L_1}\right\} \times \left\{1 - \frac{0.3x}{L_1}\right\} \tag{4.1}$$

$$A_2 = (b_2 h_2) \times \left\{1 - \frac{0.2(x - L_1)}{L_2}\right\} \times \left\{1 - \frac{0.7143(x - L_1)}{L_2}\right\} \tag{4.2}$$

Now with given boundary conditions,

Solving the equation (3.10) and(3.17) gives $C_1 = 0$

Solving the equation (3.11) and (3.16) gives C_2=0

Solving the equation (3.10), equation (3.14), and equation (3.19), (Refer chap.3)

Get the Value of $C_3 = 10.3839$

Solving the equation (3.11), equation(3.15), and equation (3.18), (Refer chap.3)

Get the Value of C_4= -0.4571

Substitute all these values in equation (3.15), (Refer chap.3)

Get the Value of y_2 = -0.0013 m

So the deflection of non-presser arm by this method = 1.3 mm.

4.5.1 Stresses In Flyer Arm

Following parameters are consider for calculate the value of factor of safety at each section.

Parameter:

N = 1200rpm

Proof stress of aluminum alloy: 175 N/mm^2

Measure and calculate parameters for each segment are tabulated below.

Table 4.3: Different parameters for each segment

Segment	Vol. 10^4 mm^4	Mass (kg)	Radius (mm)	C. force (kg)	M.I. 10^4 (mm^4)	Distance (Y) mm	Length of C.G.of segment from sections (mm)				
							Sec. B	Sec. C	Sec. D	Sec. E	Sec. F
A-B	3.86	0.10	92.7	15.50	0.782	12.66	66.5	181.9	215.4	267.5	293.5
B-C	5.12	0.14	93.8	20.94	1.89	13.77	-	54.29	88.2	140.3	166.2
C-D	2.93	0.08	94.2	12.05	3.92	14.23		-	10.77	62.86	88.8
D-E	5.6	0.15	75.8	18.39	6.94	29.4			-	16.3	42.3
E-F	6.81	0.18	51.3	15.16	9.5	21.5				-	9.76

4.6 Result Summary

The Table 4.4 shows that minimum value of factor of safety is greater than 5. Also from FE analysis the FOS is resulting as 5.240 only. Hence the optimized model is safe.

For optimized model of flyer, it is necessary to align a principal inertia axis with the geometric axis of rotation so, the centrifugal force is reduced and vibrations are minimize. Therefor in the next chapter dynamic balancing of flyer has been carried out and the same has been checked with FE analysis.

Table 4.4: Factor of safety calculation for different segments

	Section B			Section C			Section D			Section E			Section F		
Segment	Centfugal-force (N)	Length (mm)	Bending moment	Centfugal-force (N)	Length (mm)	Bending moment	Centfugal-force (N)	Length (mm)	Bending moment	Centfugal-force (N)	Length (mm)	Bending moment	Centfugal-force (N)	Length (mm)	Bending moment
A-B	152.055	66.53	10116.219	152.055	181.5	27597.983	152.055	215.4	32752.647	152.055	267.5	40674.713	152.055	293.5	44628.143
B-C				205.42	54.3	11154.306	205.42	88.2	18118.044	205.42	140.2	28799.884	205.42	166.2	34140.804
C-D							118.21	10.77	1273.1217	118.21	62.86	7430.6806	118.21	88.86	10504.141
D-E										180.4	16.3	2940.52	180.4	42.3	7630.92
E-F													148.72	9.76	1451.5072
Σ MB	Total Bending Moment @ Sec. B		10116.219	Total Bending Moment @ Sec.C		38752.289	Total Bending Moment @ Sec. D		52143.813	Total Bending Moment @ Sec. E		79845.797	Total Bending Moment @ Sec. E		98355.514
W_{xu}	Moment of resistance (I/Y)		617.69			1372.55			2754.74			2360.54			4418.6
σ_b	Total Bending Stress @ Sec. B		16.377502	Total Bending Stress @ Sec. C		28.23379	Total Bendirg Stress @ Sec. D		18.92876	Total Bending Stress @ Sec.E		33.825225	Total Bending Stress @ Sec. F		22.259429
	FOS		10.68539			6.1982468			9.2451908			5.1736537			7.8618368

Chapter 5

Design Modifications

In this chapter two plane balancing of flyer is presented. To modify the design of flyer based on size optimization, the consideration for balancing of flyer as well as for air resistance has to be kept in order to make the modifications efficient. An FE analysis under the constraint of standard operating conditions of balance model were also carried out using different material of aluminium alloys.

5.1 Introduction

Rotating machinery is commonly used in mechanical systems, including machine tools, industrial turbo-machinery, and aircraft gas turbine engines. Rotating system often produces excessive synchronous forces that reduce the life of various mechanical components. As the major area of concern is to eliminating or at least reducing unwanted inertia forces and moments to some acceptable limits. Therefore balancing is important in the manufacture and maintenance process of rotating machines. For balancing of rotating components balancing grades are referred from standard.[16]
Balancing is a technique of eliminating or at least reducing unwanted inertia forces and moments to some acceptable limits. There are many disadvantages to unbalanced systems.(Unbalance happens because the densities of materials are uneven) When a system is rotating with unbalanced masses unnecessary vibration occurs, further it

may generate unwanted noise, excessive stresses in machine elements and reduce the reliability for the all parts associated with the rotating system.
When several masses rotate in single plane, the system is said to be statically balanced if the vector sum of all forces are zero. Several masses rotate in different planes, the system is subjected to two types of unbalance (centrifugal force and couple), such type of balancing is often called dynamic balancing.

5.2 Dynamic Balancing of Flyer

For optimized model of flyer, it is necessary to align a principal inertia axis with the geometric axis of rotation through addition or removal of material. In order to reduce centrifugal forces and hense vibration. The flyer is rotating along the Z-direction as per the reference frame of solid modeling software, hence it has to be checked for distribution of unbalance mass in X and Y direction. The magnitude of unbalance will be a function of the angle between the axes and the distance of the origin (mass center) from the axis of rotation. For evaluating the distribution of unbalanced mass with respect to rotational axis, the flyer assembly is divided into four quadrants with respect to axis as shown in Figure 5.1. Figure 5.2 shows unbalance mass distance of the origin from the axis of rotation. As the different masses rotate in different planes so dynamic balancing is necessary. Calculation for position of mass and angular position of mass at each quadrant is listed in Table. 5.1

The two plane dynamic balancing method is to be planned to evaluate unbalance mass and angular position of mass suggesting modifications of the present design of the flyer. The FE analysis has been carried out to check modified design of flyer for deformation and von-Mises stresses within operating conditions. The same approach can be used to compare and evaluate different designs of the modification of flyer.
The process of getting the finalized design of the modification of the flyer is an iterative process. These iterations are done using two plane balancing method and the

simulation with the help of finite element analysis tools. The process of modification involves the fulfillment of the requirements of balancing quality grade standards as well as structural point of view.

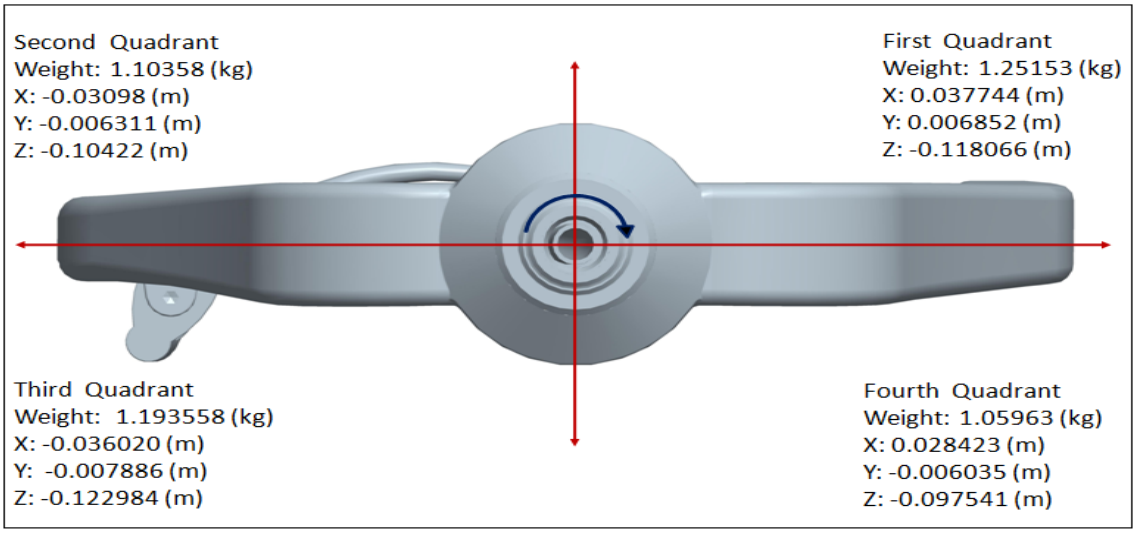

Figure 5.1: Top view of flyer assembly

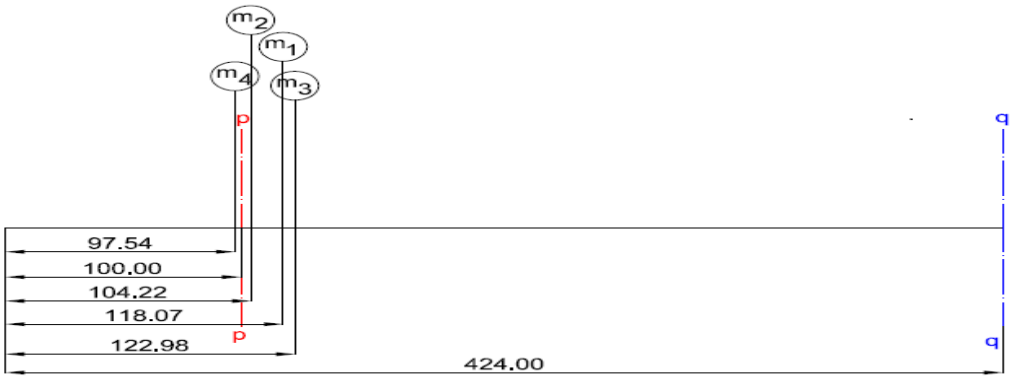

Figure 5.2: Distance of unbalance mass from the origin

Table 5.1: Location of mass at each quadrant

Quad-rant	Weight (kg)	C.G.			R=$\sqrt{x^2+y^2}$	θ= $\tan^{-1}$(Y/X)
		X(m)	Y(m)	Z(m)		
1	1.251553	0.0377444	0.0068524	-0.1180664	0.038361	10.2856
2	1.103585	-0.030984	0.0063115	-0.1042208	0.031620	-11.5136
3	1.193558	-0.036204	-0.00788605	-0.1229848	0.037053	12.2882
4	1.059626	0.0284234	-0.00603502	-0.0975411	0.029057	-11.9825

5.3 Two Plane Balancing of Flyer

Two plane balancing in which unbalanced centrifugal forces and couples are resolved in horizontal and vertical directions. Effects of rotating masses are transferred to the two arbitrarily chosen reference planes. Selection of reference plane is based on the shape of geometry. As shown in Figure 5.2 reference plane pp at a distance 100mm from origin of geometry, and Reference plane qq at the end of flyer arm.

Let, m_p = balancing mass put up on the plane pp at a radius r_p

m_q = balancing mass put up on the plane qq at a radius r_q

Reference planes become dynamically balanced when it satisfies the following necessary and sufficient conditions.[17],[18]

1) Vector sum of centrifugal forces must be equal to zero.

2) Vector sum of couples must be zero.

First resolve the Horizontal component of unbalance couple

$$\sum_{i=1}^{n} m_i r_i l_i cos\theta_i + m_q r_q l_q cos\theta_q = 0 \tag{5.1}$$

Vertical component of unbalance couple

$$\sum_{i=1}^{n} m_i r_i l_i sin\theta_i + m_q r_q l_q sin\theta_q = 0 \tag{5.2}$$

Solve equation (5.1) and (5.2) find the magnitude of balancing couple as,

$$m_q r_q l_q = \sqrt{(\sum_{i=1}^{n} m_i r_i l_i cos\theta_i)^2 + (\sum_{i=1}^{n} m_i r_i l_i sin\theta_i)^2} \tag{5.3}$$

Angular position of mass m_q

$$tan\theta_q = \frac{-\sum_{i=1}^{n} m_i r_i l_i sin\theta_i}{-\sum_{i=1}^{n} m_i r_i l_i cos\theta_i} \tag{5.4}$$

After knowing the values of balancing mass m_q and its angular position θ_q from above equations, resolve the centrifugal forces in horizontal and vertical directions equate them to zero. Refer Table 5.2 and 5.3 for calculation of horizontal and vertical component of couple and force respectively.

Horizontal component of unbalance force

$$\sum_{i=1}^{n} m_i r_i cos\theta_i + m_q r_q cos\theta_q + m_p r_p cos\theta_p = 0 \tag{5.5}$$

Vertical component of unbalance force

$$\sum_{i=1}^{n} m_i r_i sin\theta_i + m_q r_q sin\theta_q + m_p r_p sin\theta_p = 0 \tag{5.6}$$

Solve equation (5.5) and (5.6) find the magnitude of balancing force

$$m_p r_p = \sqrt{(\sum_{i=1}^{n} m_i r_i cos\theta_i + m_q r_q cos\theta_q)^2 + (\sum_{i=1}^{n} m_i r_i sin\theta_i + m_q r_q sin\theta_q)^2} \tag{5.7}$$

Angular position of mass m_p

$$tan\theta_p = \frac{-(\sum_{i=1}^{n} m_i r_i sin\theta_i + m_q r_q sin\theta_q)}{-(\sum_{i=1}^{n} m_i r_i cos\theta_i + m_q r_q cos\theta_q)} \tag{5.8}$$

Table 5.2: Horizontal and vertical component of couple

Plane	**Mass (m)**	**Radius (r)**	**Mass radius ($m \times r$)**	**Distance from ref plane 'p'=(l)**	**Mass Radius length =(mrl)**	**(mrl)cosθ**	**(mrl)sinθ**
p	m_p	r_p	$m_p \times r_p$	0	0	-	-
1	1.25155	0.0383614	0.048011	0.018066	0.0008673	-0.000853	-0.000153
2	1.10358	0.0316203	0.034896	0.004220	0.000147	0.0001442	-2.96E-5
3	1.19355	0.0370533	0.044225	0.022984	0.0010165	0.0009934	-0.000215
4	1.05962	0.0290571	0.030789	-0.002458	-7.570 e-5	7.403 e-5	-1.581 e-5
q	m_q	r_q	$m_q \times r_q$	0.324	$m_q \times r_q \times$ 0.324		

Table 5.3: Horizontal and vertical component of force

Plane	**Mass (m)**	**Radius (r)**	**Mass radius ($m \times r$)**	**Distance from ref plane 'p' = (l)**	**(mr)cosθ**	**(mr)sinθ**
p	m_p	r_p	$m_p \times r_p$	0	-	-
1	1.25155	0.0383614	0.0480113	0.018066	0.0472392	0.00857
2	1.10358	0.0316203	0.0348957	0.004220	-0.0341935	0.00696
3	1.19355	0.0370533	0.0442253	0.022984	-0.0432120	-0.00941
4	1.05962	0.0290571	0.0307896	-0.002458	0.0301182	-0.00639
q	m_q	r_q	0.0011065	0.324	0.001105	5.024 e-5

5.4 First Design Modification

The concept of reducing unbalance mass of assemblies of flyer, the modification which is used in the flyer. The modification has been done by changing the depth of flyer

cross-section at the middle as well as the end of non-presser arm. The static structural FE analysis has been carried out maintaining the condition of the constraints same as that of the reference condition to evaluate the modification. The solution has been obtained for total displacement and von-Mises stress distribution of first modification model. Deflection and the von-Mises stress plots for flyer arm are shown in Figure 5.3 and Figure 5.4 respectively.

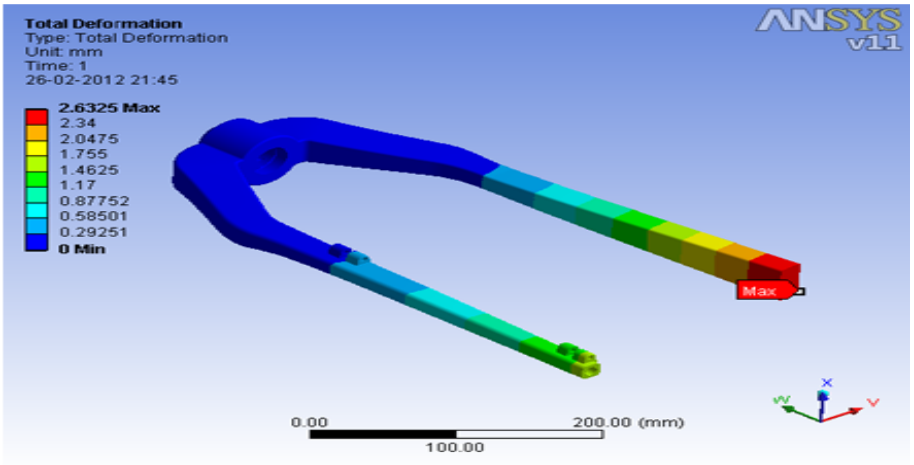

Figure 5.3: Total deformation in first modified design of flyer

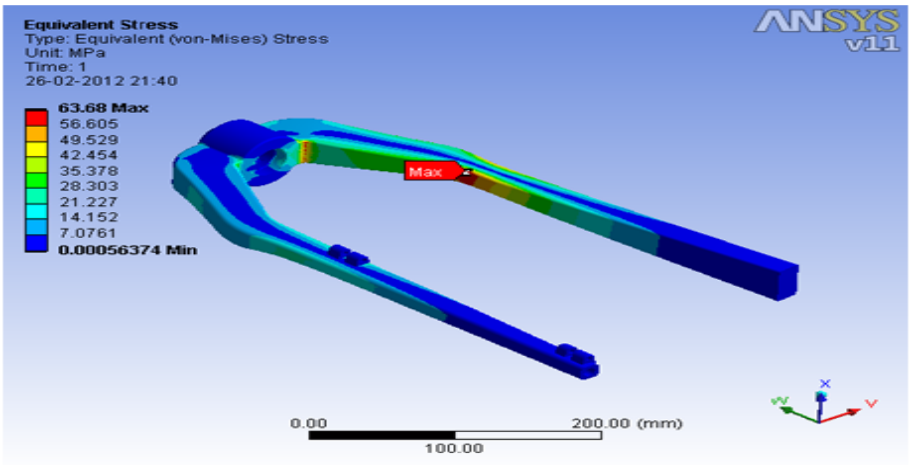

Figure 5.4: von-Mises stress on first modified design of flyer

5.4.1 Result Summary for First Design Modification

- At a distance 100 mm from origin, unbalance mass is 783.098 gram.mm, which is obtained at an angle 177.397 degree. (i.e. in second quadrant)
- At the end of solid arm unbalance mass is 439.879 gram.mm, which is obtained at an angle -294.586 degree. (i.e. in first quadrant)
- The maximum deflection and von-Mises stress in flyer arm are 2.6325 mm and 63.68 MPa respectively.
- For the modified design FOS is less than 3, hence further modification in geometry is required.

5.5 Second Design Modification

The concept of reducing unbalance mass of assemblies of flyer, the modification which is used in the flyer. The modification has been done by increasing the length of non-presser arm of flyer. The static structural FE analysis has been carried out maintaining the condition of the constraints same as that of the reference condition to evaluate the modification. The solution has been obtained for total displacement and von-Mises stress distribution of second modification model. Deflection and the von-Mises stress plots for flyer arm are shown in Figure 5.5 and Figure 5.6 respectively.

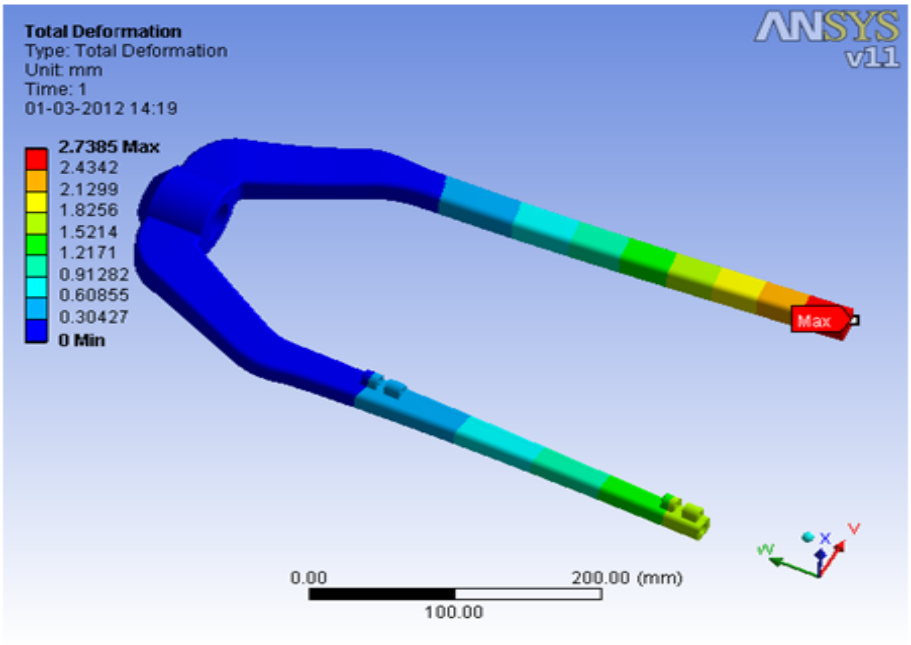

Figure 5.5: Total deformation in second modified design of flyer

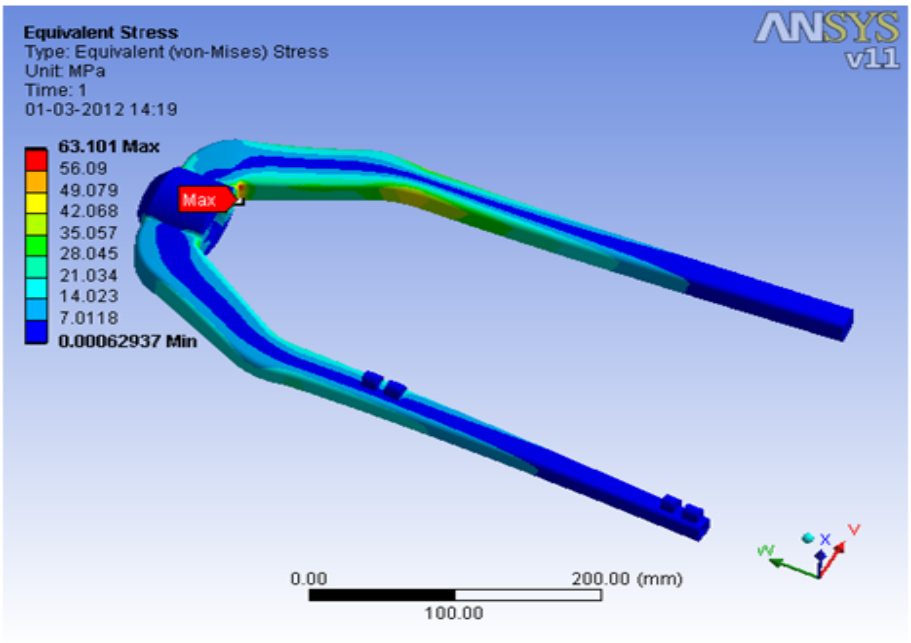

Figure 5.6: von-Mises stress on second modified design of flyer

5.5.1 Result Summary of Second Design Modification

- At a distance 100 mm from origin, unbalance mass is 817.953 gram.mm, which is obtained at an angle 177.397 degree. (i.e. in second quadrant)
- At the end of solid arm unbalance mass is 1077.191 gram.mm, which is obtained at an angle -357.038 degree. (i.e. in first quadrant)
- The maximum deflection and von-Mises stress in flyer arm are 2.7385 mm and 63.101 MPa respectively.
- For the modified design FOS is less than 3, hence further modification in geometry is required.

5.6 Third Design Modification

The concept of reducing unbalance mass of assemblies of flyer, the modification which is used in the flyer. The modification has been done by changing the depth of flyer cross-section at the middle as well as the end of non-presser arm. The static structural FE analysis has been carried out maintaining the condition of the constraints same as that of the reference condition to evaluate the modification. The solution has been obtained for total displacement and von-Mises stress distribution of third modification model. Deflection and the von-Mises stress plots for flyer arm are shown in Figure 5.7 and Figure 5.8 respectively.

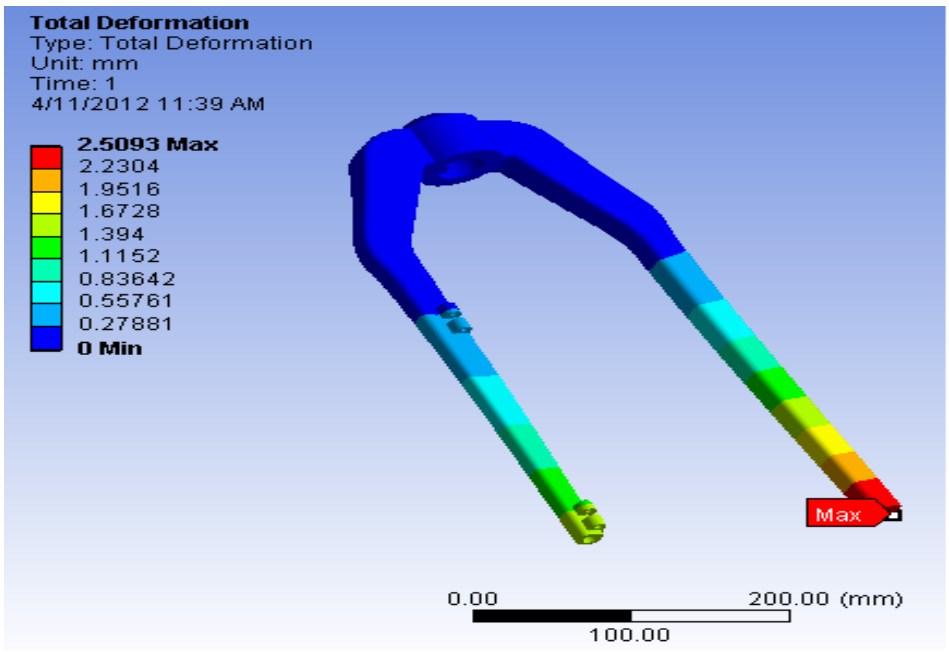

Figure 5.7: Total deformation in third modified design of flyer

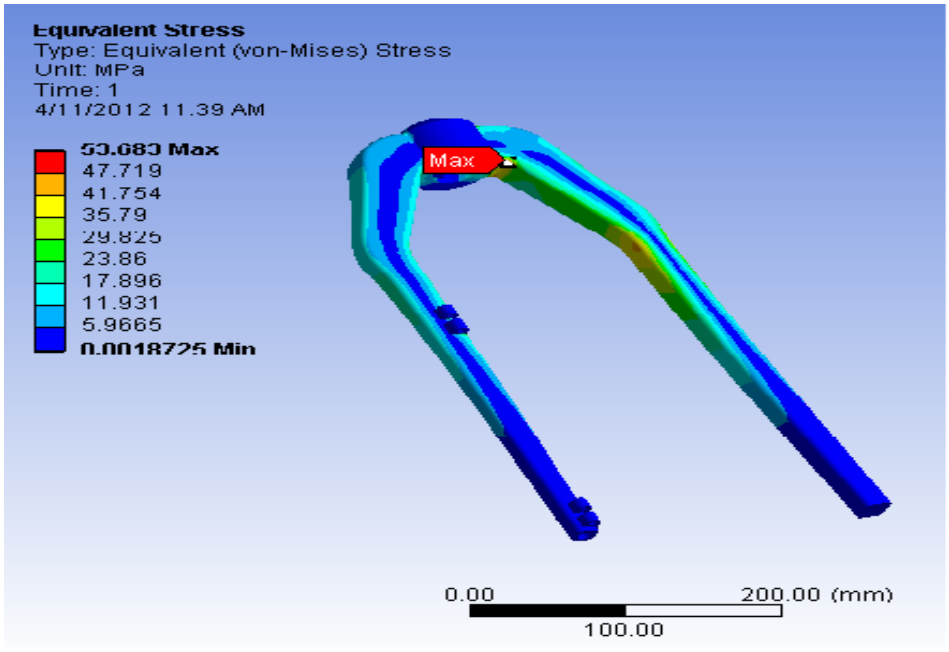

Figure 5.8: von-Mises stress on third modified design of flyer

5.6.1 Result Summary of Third Design Modification

- At a distance 100 mm from origin, unbalance mass is 1079.062345 gram.mm, which is obtained at an angle 168.40 degree. (i.e. in second quadrant)
- At the end of solid arm unbalance mass is 1106.581639 gram.mm, which is obtained at an angle -357.25 degree. (i.e. in first quadrant)
- The maximum deflection and von-Mises stress in flyer arm are 2.492 mm and 57.189 MPa respectively.
- The value of von-Mises stresses are lower, so the FOS more than 3 so the design modification is not require.

5.7 Final Modification Considering Dynamic Balancing

From the result of balancing and FE analysis, modified 3D solid model of flyer is prepared in pro/e. as shown in Figure 5.9.

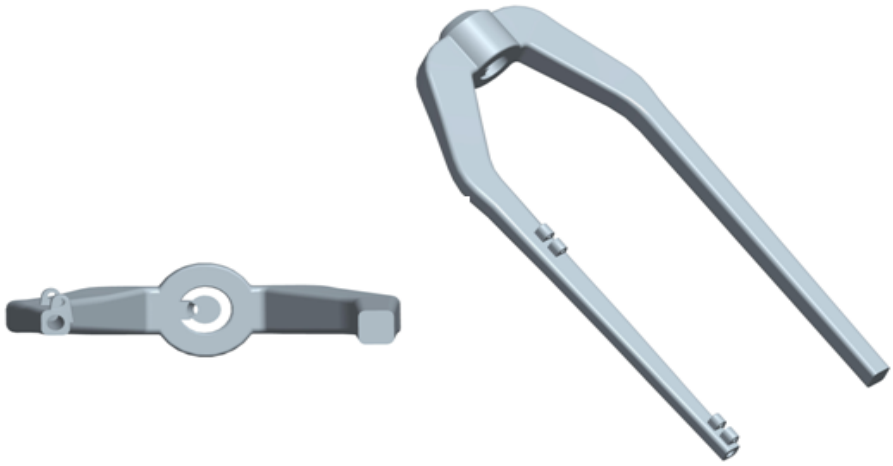

Figure 5.9: Redesign of flyer

5.8 Deflection of Flyer Arm for Balanced Model

From the basic of solid mechanics, as explained in section 3.2 and 3.3 deflection at the end of flyer arm and stresses at various segment are obtained as shown in Figure 3.5 and Table 5.4 and 5.5 respectively.

Parameter

ρ_{Al}=2700 kg/m^3 ; R=0.09 m ; ω=125.6 rad/s

b_1 = 0.043 m ; h_1 = 0.03 m ; L_1 = 0.112 m

b_2 = 0.025 m ; h_2 = 0.024 m ; L_2 = 0.312 m

E=7.1 GPA ; $I_1 = 3.125\ e^{-8}m^4$; $I_2 = 1.43\ e^{-8}m^4$

$$A_1 = (b_1 h_1) \times \left\{1 - \frac{0.419x}{L_1}\right\} \times \left\{1 - \frac{0.2x}{L_1}\right\} \tag{5.9}$$

$$A_2 = (b_2 h_2) \times \left\{1 - \frac{0.104(x - L_1)}{L_2}\right\} \times \left\{1 - \frac{0.2(x - L_1)}{L_2}\right\} \tag{5.10}$$

Now with given boundary conditions,

Solving the equation (3.10) and(3.17) gives $C_1 = 0$

Solving the equation (3.11) and (3.16) gives C_2=0

Solving the equation (3.10), equation (3.14), and equation (3.19), (Refer chap.3)

Get the Value of C_3 = 8.8383

Solving the equation (3.11), equation(3.15), and equation (3.18), (Refer chap.3)

Get the Value of C_4= -0.4194

Substitute all these values in equation (3.15), (Refer chap.3)

So the deflection of non-presser arm by this method = 2.7 mm.

5.8.1 Stress in Flyer Arm

Following parameters are consider for calculate the value of factor of safety at each section.

N = 1200rpm

Proof stress of aluminum alloy: 175 N/mm^2

Measure and calculate parameters for each segment are tabulated below.

Table 5.4: Different parameters for each segment

Segment	Vol. 10^4 mm^4	Mass (kg)	Radius (mm)	C. force (kg)	M.I. 10^4 (mm^4)	Distance (Y) mm	Length of C.G.of segment from sections (mm)				
							Sec. B	Sec. C	Sec. D	Sec. E	Sec. F
A-B	9.145	0.25	93.0	37.04	2.887	11.54	86.83	200.1	250.8	300.9	326.9
B-C	5.635	0.15	93.0	22.13	3.215	12.49	-	53.49	104.2	154	180.3
C-D	3.676	0.10	93.2	14.93	2.3751	13.5		-	20.19	70.32	96.44
D-E	5.630	0.15	75.2	18.45	9.85	19.5			-	23.13	42.42
E-F	6.784	0.18	51.2	15.14	9.4	21.5				-	9.71

The Table 5.4 shows that minimum value of factor of safety is greater than 5 at each segment, hence the new model is safe.

Table 5.5: Factor of safety calculation for different segments

	Section B			Section C			Section D			Section E			Section F		
Segment	Centfugal force (N)	Length (mm)	Bending moment	Centfugal force (N)	Length (mm)	Bending moment	Centfugal force (N)	Length (mm)	Bending moment	Centfugal force (N)	Length (mm)	Bending moment	Centfugal force (N)	Length (mm)	Bending moment
A-B	363.36	86.8	31539.648	363.36	201.3	73144.368	363.36	250.8	91130.688	363.36	300.9	109335.024	363.36	326.9	118782.384
B-C				223.96	53.5	11981.86	223.96	104.2	23336.632	223.96	154.3	34557.028	223.96	180.3	40379.988
C-D							146.46	20.2	2958.492	146.46	70.3	10296.138	146.46	96.4	14118.744
D-E										180.99	23.1	4180.869	180.99	42.4	7673.976
E-F													148.52	9.7	1440.644
Σ MB	Total Bending Moment @ Sec. B		31539.648	Total Bending Moment @ Sec.C		85126.228	Total Bending Moment @ Sec. D		117425.812	Total Bending Moment @ Sec. E		158369.059	Total Bending Moment @ Sec. E		182395.736
W_{zu}	Moment of resistance (IIY)		2501.73			2574.06			2349.14			5051.28			4372.09
σ_b	Total Bending Stress @ Sec. B		12.6073351	Total Bending Stress @ Sec. C		33.07008018	Total Bending Stress @ Sec. D		49.98867237	Total Bending Stress @ Sec.E		31.352263	Total Bending Stress @ Sec. F		41.71822025
	FOS		13.88102284			5.29167697			3.500932959			5.591734425			4.1946116

5.9 Air Resistance of Proposed Geometry

In fluid dynamics, drag also called air resistance refers to forces which act on a solid object in the direction of the relative fluid flow velocity. Drag coefficient (denoted as: C_d) is a dimensionless quantity that is used to quantify the drag or resistance of an object in a fluid environment such as air or water. The drag coefficient is always associated with a particular surface area. C_d is not a constant but varies as a function of speed, flow direction, object position, object size, fluid density and fluid viscosity. The affect of air resistance depends upon three things: the mass of the object, the size (area) of the object and the speed of the object. It is generated by the interaction and contact of a solid body with a fluid (liquid or gas). For drag to be generated, the solid body must be in contact with the fluid. Drag is generated by the difference in velocity between the solid object and the fluid. There must be motion between the object and the fluid.[19],[20]

5.9.1 Theoretical Drag Force Calculation

$$F = 0.5 C_d \rho A V^2 [19] \tag{5.11}$$

$$= 0.462N$$

Where,

A = Reference area (m^2)

C_d = Drag coefficient

F = Drag force (N)

V = Velocity (m/s)

ρ= Density of fluid (kg/m^3)

5.9.2 FE Analysis for Drag Force

The solid model of proposed geometry is prepared in NX7 as shown in Figure 5.10 and mesh in Gambit. When the full volume has been meshed as shown in Figure 5.11, boundary conditions are given to the geometry, where top, bottom, left and right side of the geometry are given to the symmetry and velocity inlet of air 11.304 m/s was applied to the frontal area of geometry and back face is given to outlet as shown in Figure 5.10. The FE model was applied to solver and the solution has been obtained. Drag co-efficient plot for the proposed geometry is shown in Figure 5.12.

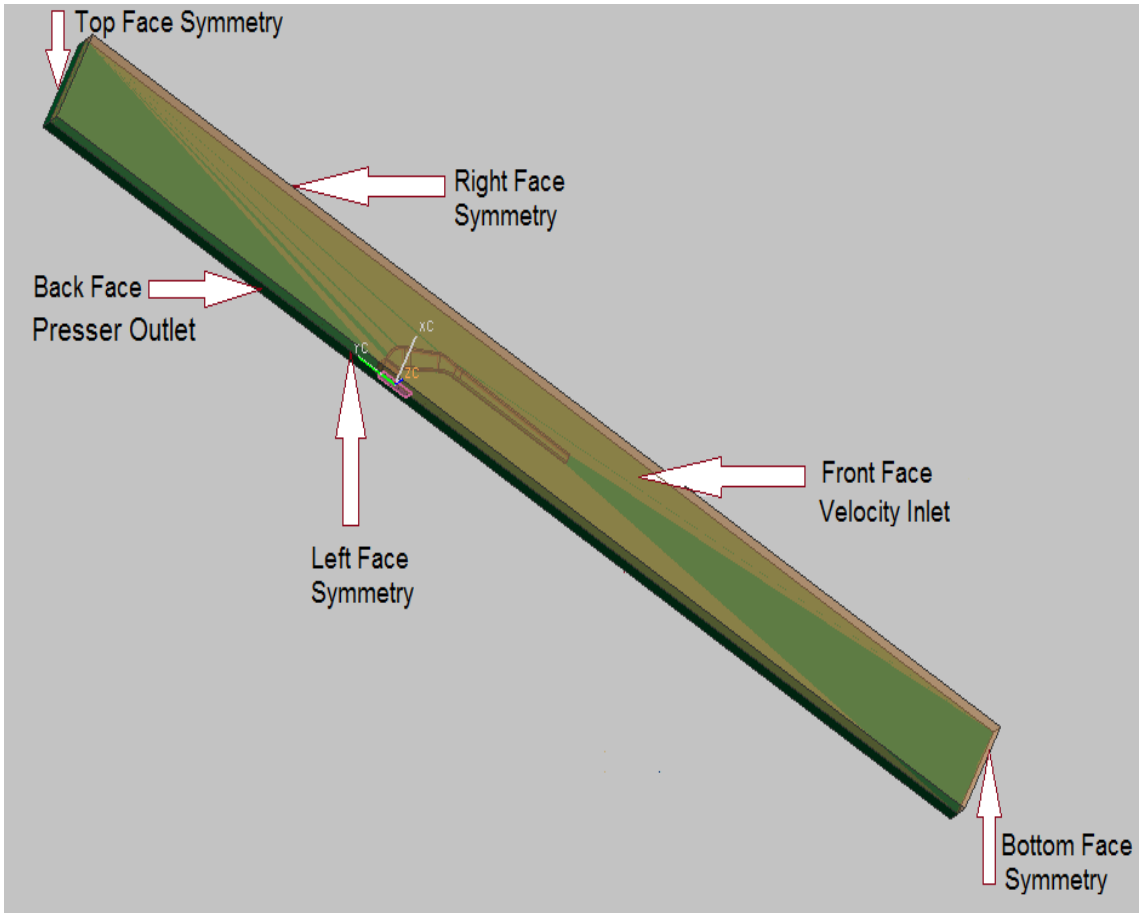

Figure 5.10: solid model of proposed geometry

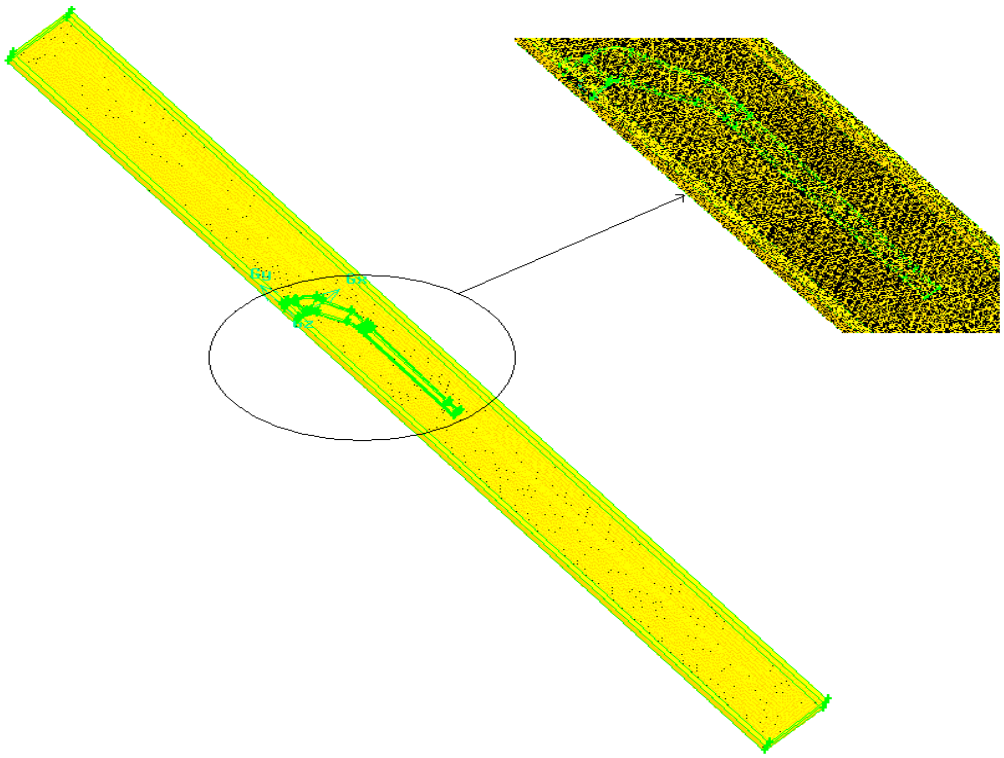

Figure 5.11: Mesh model of proposed geometry

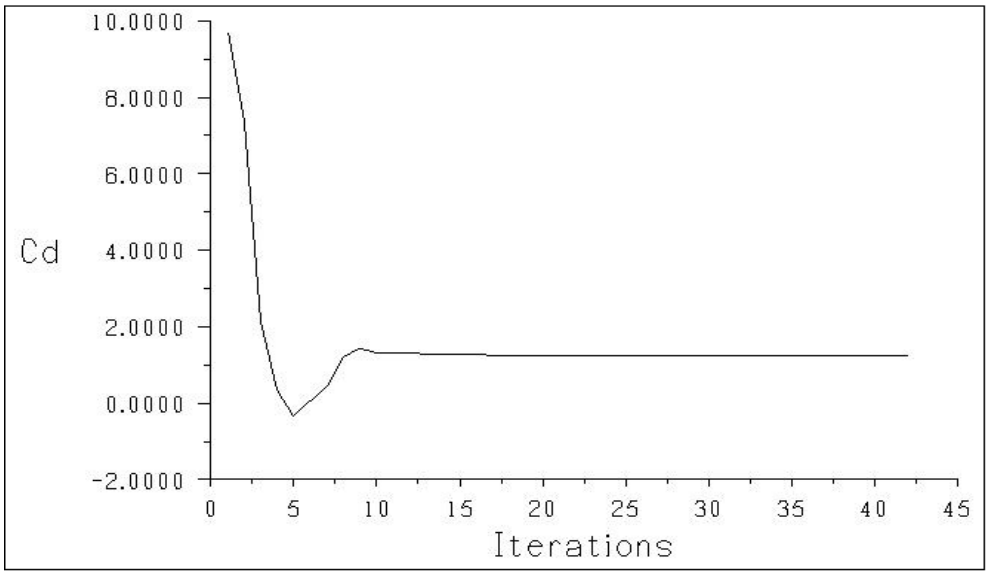

Figure 5.12: Drag co-efficient

From the FE analysis carried out the drag coefficient and drag force are stated below:
Maximum drag-coefficient is 1.24
Maximum drag force 0.761 N

5.10 Design for Alternate Material

Existing flyer is made from die casting process, for die casting process various non-ferrous materials are use like aluminium, magnesium, zinc, copper, etc. Aluminum die casting alloys are lightweight, offer good corrosion resistance, ease of casting, good mechanical properties and dimensional stability. Aluminum alloy A380, 383, 413, 518, B390 are used for die casting process. Their mechanical properties and chemical composition are shown in Table 5.6 and 5.7 respectively.

Table 5.6: Mechanical properties of aluminum alloy[21]

Mechanical properties	**A380**	**383**	**413**	**518**	**B390**
Ultimate tensile strength(MPa)	320	310	300	310	320
Yield strength (MPa)	160	150	140	190	250
Young Modulus (MPa)	71000	71000	71000	71000	81300
Density (kg/m3)	2.71	2.74	2.66	2.57	2.73
Poisson's ratio	0.33	0.33	0.33	0.33	0.33

Table 5.7: Chemical composition of aluminum alloy[21]

Composition	**A380**	**383**	**413**	**518**	**B390**
Silicon (Si)	7.5-9.5	9.5-11.5	11.0-13.0	0.35	16.0-18.0
Iron (Fe)	1.3	1.3	2.0	1.8	1.3
Copper (Cu)	3.0-4.0	2.0-3.0	1.0	0.25	4.0-5.0
Manganese (Mn)	0.50	0.50	0.35	0.35	0.50
Magnesium (Mg)	0.10	0.10	0.10	7.5-8.5	0.45-.65
Nickel (Ni)	0.5	0.30	0.50	0.15	0.10
Zinc (Zn)	3.0	3.0	0.50	0.15	1.5
Tin (Sn)	0.35	0.15	0.15	0.15	—
Titanium (Ti)	—	—	—	—	0.10
Others	0.50	0.50	0.25	0.25	0.20
Aluminium (Al)	Balance	Balance	Balance	Balance	Balance

5.10.1 Aluminium Alloy A380

Considering the same boundary condition of existing flyer, the static structural analysis has been done for aluminium alloy A380 and the plot for deflection and maximum von-Mises stresses are obtained as shown in Figure 5.13 and Figure 5.14 respectively.

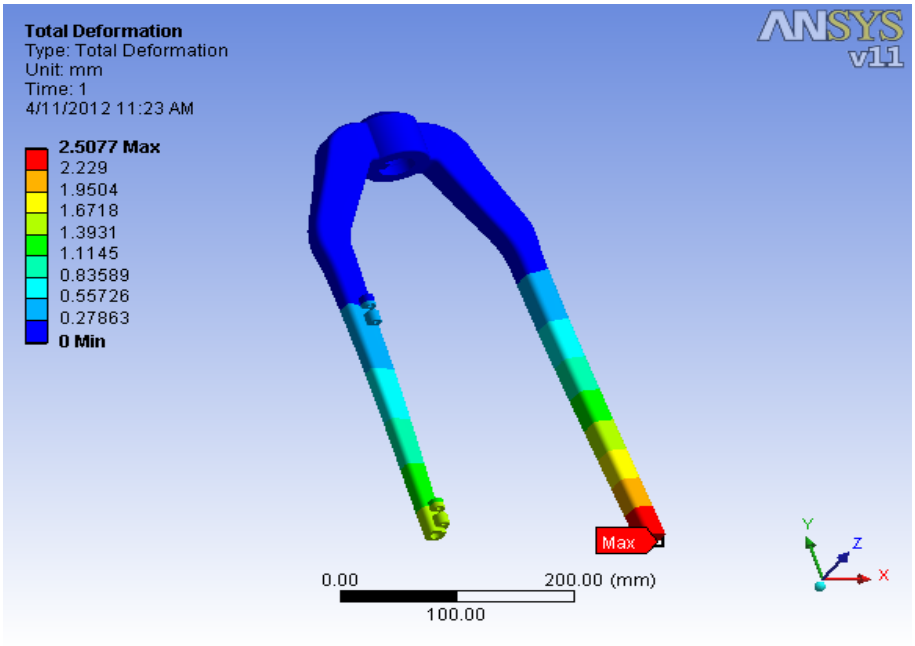

Figure 5.13: Total deformation for aluminium alloy A380

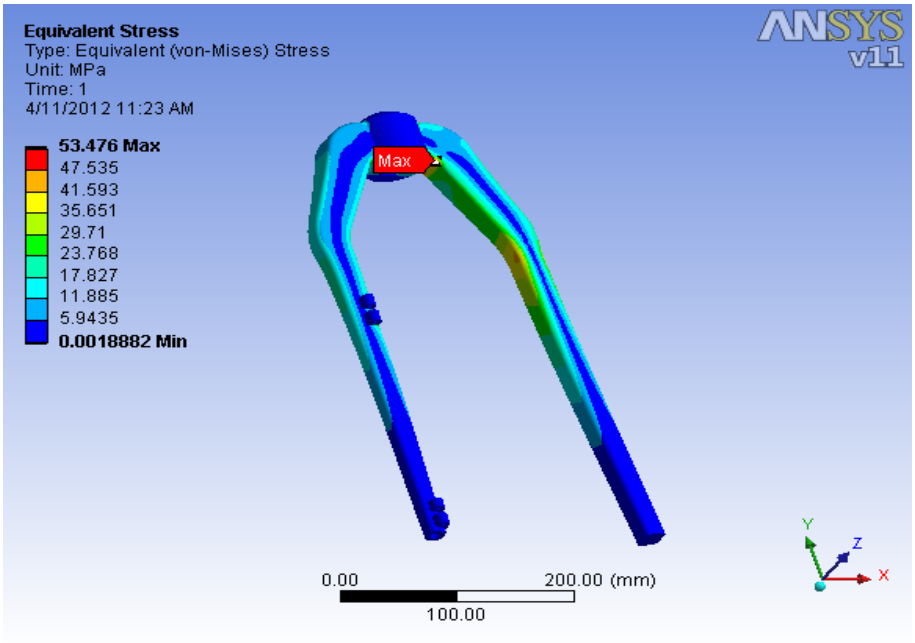

Figure 5.14: von-Mises Stress for aluminium alloy A380

5.10.2 Aluminium Alloy 383

Considering the same boundary condition of existing flyer, the static structural analysis has been done for aluminium alloy 383 and the plot for deflection and maximum von-Mises stresses are obtained as shown in Figure 5.15 and Figure 5.16 respectively.

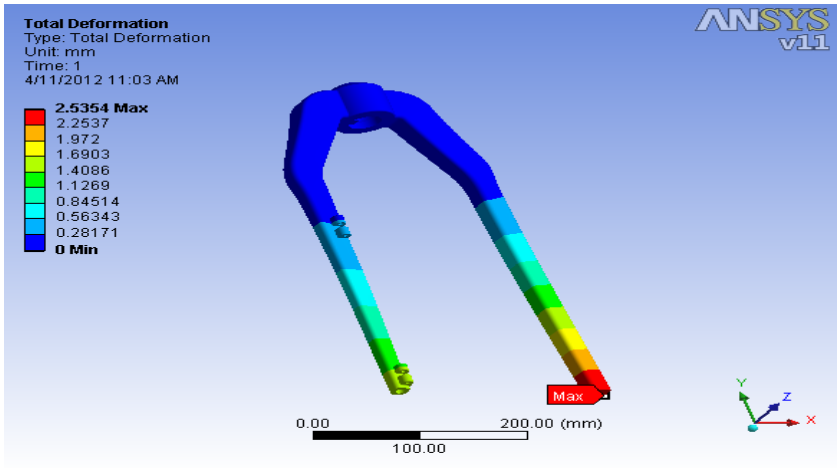

Figure 5.15: Total deformation for aluminium alloy 383

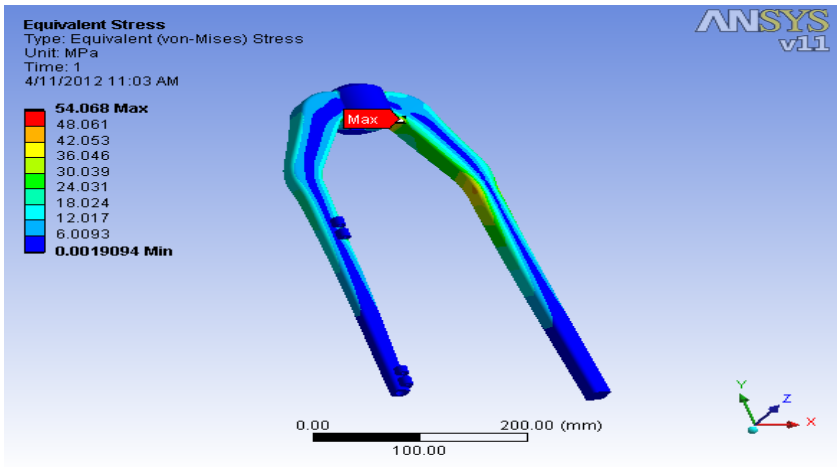

Figure 5.16: von-Mises stress for aluminium alloy 383

5.10.3 Aluminium Alloy 413

Considering the same boundary condition of existing flyer, the static structural analysis has been done for aluminium alloy 413 and the plot for deflection and maximum von-Mises stresses are obtained as shown in Figure 5.17 and Figure 5.18 respectively.

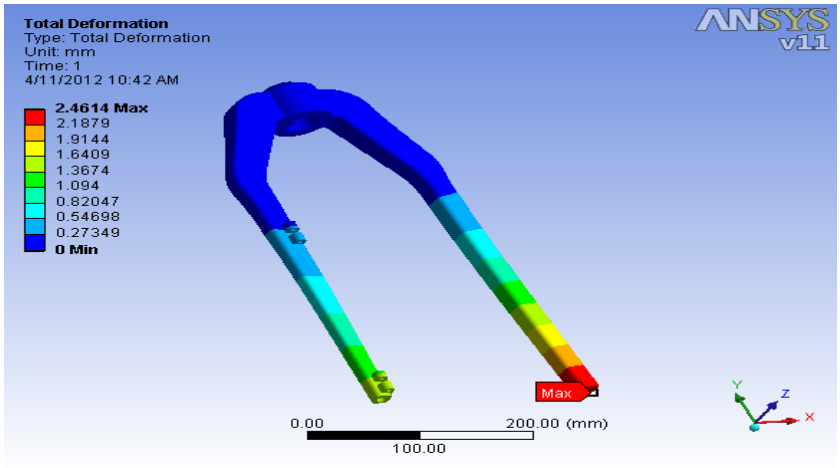

Figure 5.17: Total deformation for aluminium alloy 413

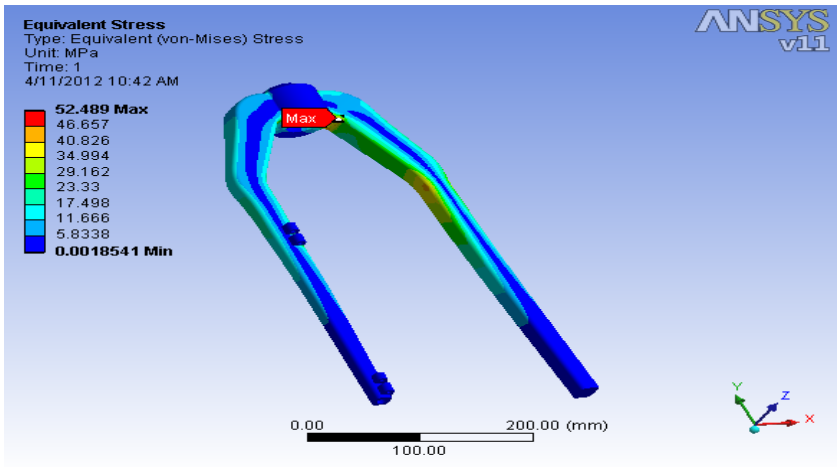

Figure 5.18: von-Mises stress for aluminium alloy 413

5.10.4 Aluminium Alloy 518

Considering the same boundary condition of existing flyer, the static structural analysis has been done for aluminium alloy 518 and the plot for deflection and maximum von-Mises stresses are obtained as shown in Figure 5.19 and Figure 5.20 respectively.

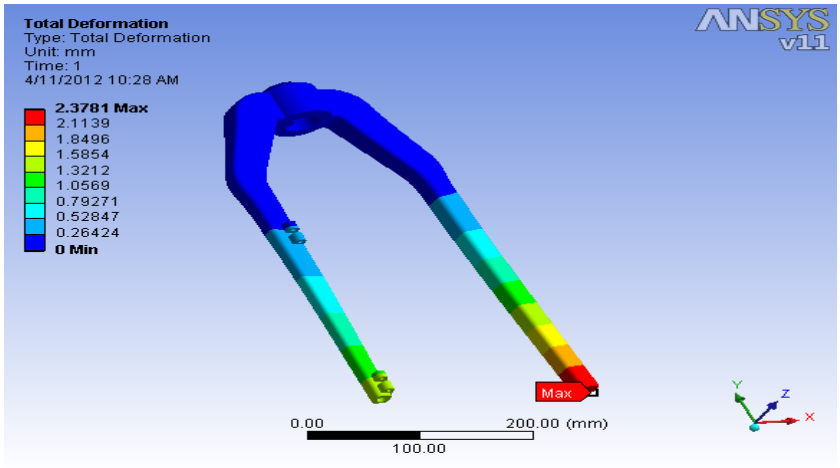

Figure 5.19: Total deformation for aluminium alloy 518

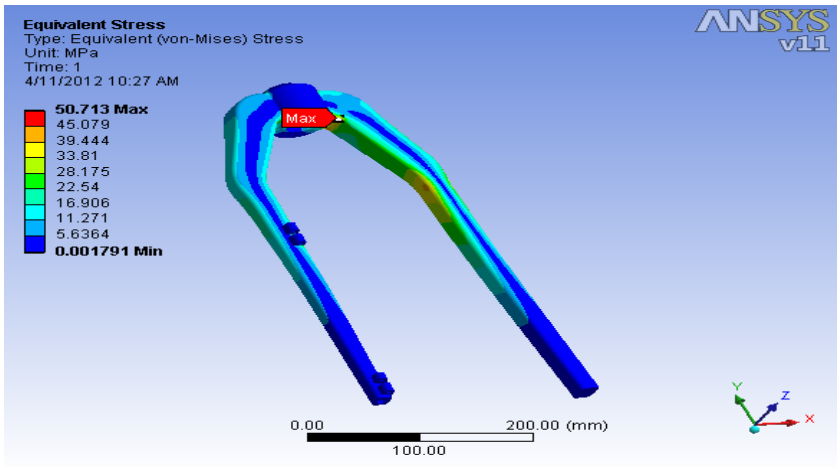

Figure 5.20: von-Mises stress for aluminium alloy 518

5.10.5 Aluminium Alloy B390

Considering the same boundary condition of existing flyer, the static structural analysis has been done for aluminium alloy B390 and the plot for deflection and maximum von-Mises stresses are obtained as shown in Figure 5.21 and Figure 5.22 respectively.

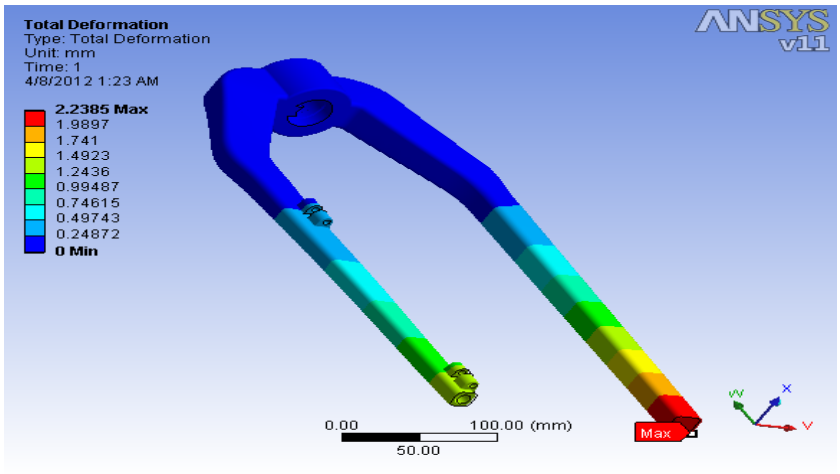

Figure 5.21: Total deformation for aluminium alloy B390

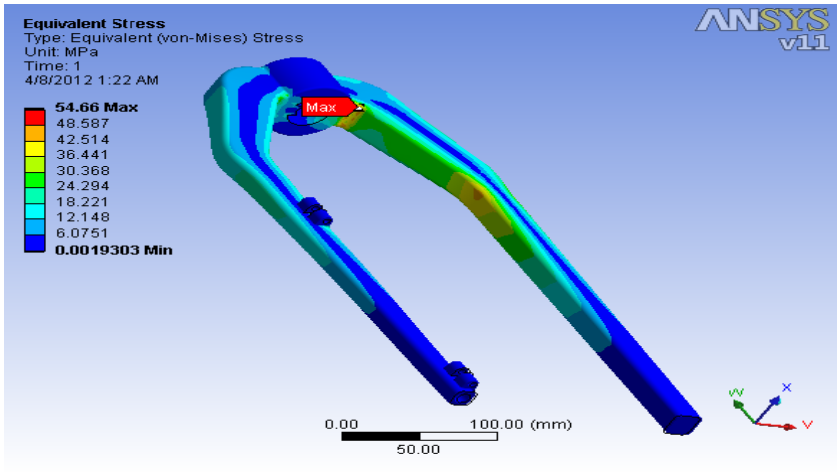

Figure 5.22: von-Mises stress for aluminium alloy B390

Design for alternate material following results are obtained from FE Analysis.

Table 5.8. shows the deflection, von-Mises stresses and factor of safety for different aluminium alloy. The FOS for aluminium alloy 518 and B390 are within the limit of constraint, so this two materials can be used for the realization of optimized balanced model.

Table 5.8: Result of analysis of flyer for different material

Material	Deflection (mm)	von-Mises stress (MPa)	FOS
A380	2.5077	53.476	2.99
383	2.5354	54.068	2.77
413	2.4614	52.489	2.66
518	2.3781	50.713	3.74
B390	2.2385	54.66	4.57

Chapter 6

Result and Discussion

In this chapter results obtained from the static analysis, size optimization, dynamic balancing, air resistance and design for alternate material of flyer has been discussed.

6.1 Deflection and Stresses for Existing model of Flyer

The FEA results of deflection and von-Mises stress profiles of original configuration for the flyer is shown in Figure 6.1 and 6.2 respectively. The maximum deflection and von-Mises stress in flyer arm are 2.654 mm and 53.739 MPa respectively. The FE analysis shows the location of the maximum von Mises stresses near the junction of the arm and the shaft locating hub, as the geometry is constrained near the hub portion. The free end of the flyer arm deflects maximum as that end being the free end. Also the theoretical analysis has been carried out in Chapter 3. The comparison for deflection obtained with theoretical analysis and FE analysis is given in Table 6.1.

Table 6.1: Deflection at free end of flyer

Sr.No.	Method	Deflection (mm)
1	Theoretical analysis	1.9
2	FE Analysis	2.6574
3	% reduction	28.50

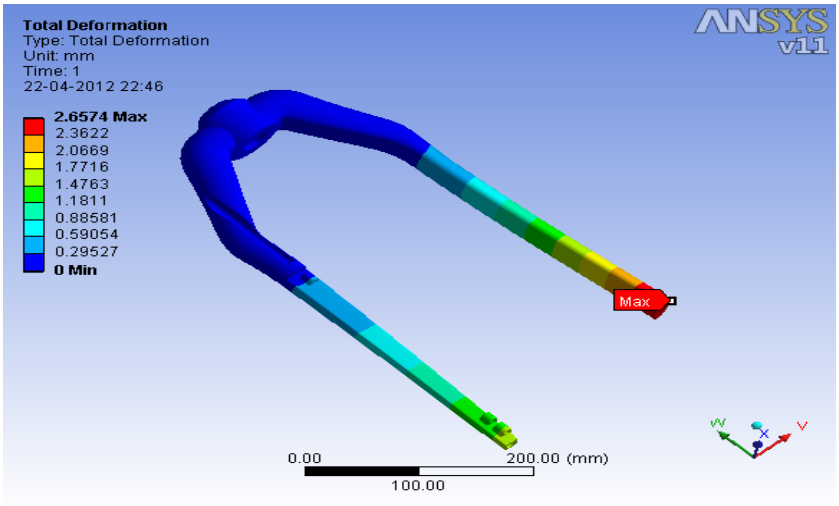

Figure 6.1: Total deformation of existing flyer

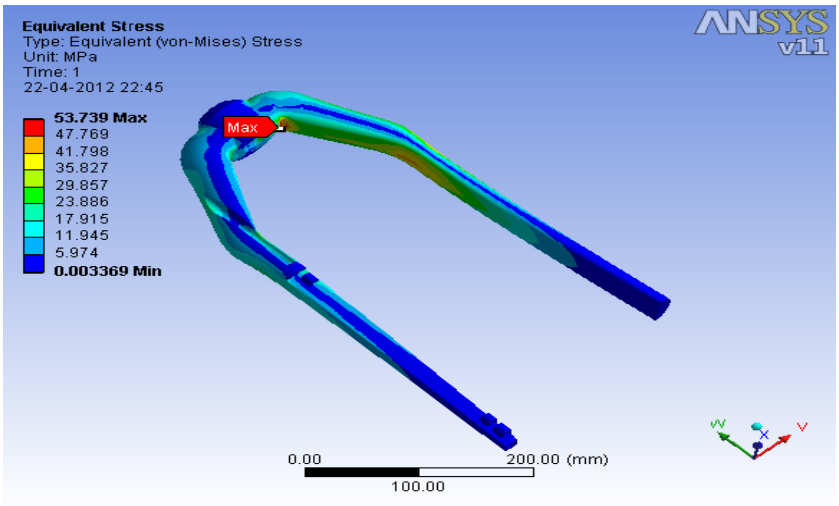

Figure 6.2: von-Mises stress on existing flyer

6.2 Deflection and Stresses for Optimized model of Flyer

The FEA results of deflection and von-Mises stress profiles of original configuration for the flyer is shown in Figure 6.3 and 6.4 respectively. The maximum deflection and von-Mises stress in flyer arm are 1.3237 mm and 33.56 MPa respectively. The FE analysis shows the location of the maximum von Mises stresses near the junction of the arm and the shaft locating hub, as the geometry is constrained near the hub portion. The free end of the flyer arm deflects maximum as that end being the free end. Also the theoretical analysis has been carried out in Chapter 4. The comparison for deflection obtained with theoretical analysis and FE analysis is given in Table 6.2.

Table 6.2: Deflection at free end of flyer

Sr.No.	Method	Deflection (mm)
1	Theoretical analysis	1.3
2	FE Analysis	1.3237
3	% reduction	1.79

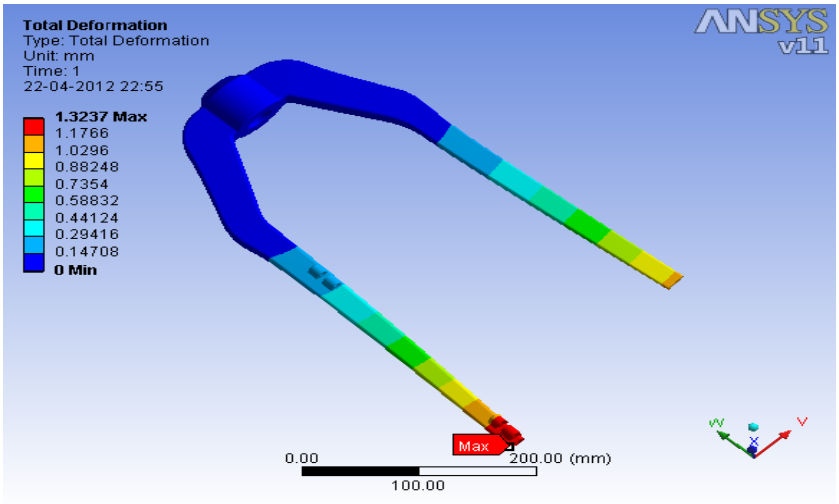

Figure 6.3: Total deformation of optimized model of flyer

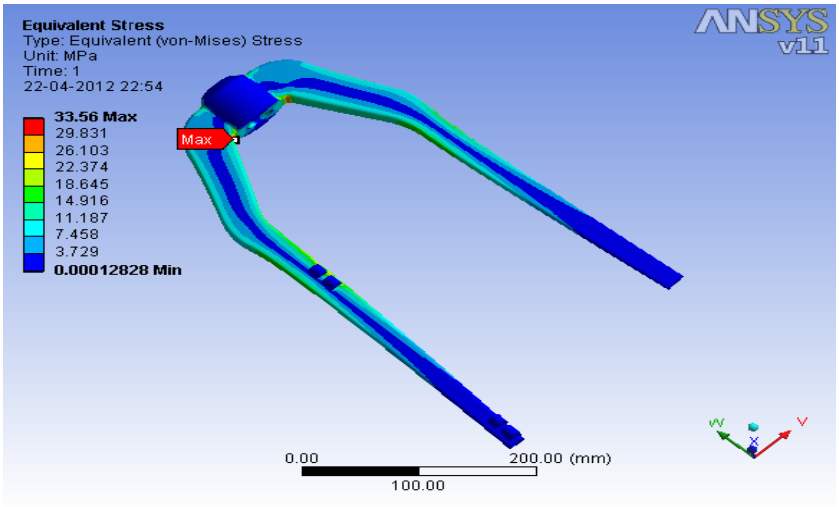

Figure 6.4: von-Mises stress on optimized model of flyer

6.3 Balancing Result

The result of two plane balancing method, magnitude and angular position of mass is obtained in two reference planes p and q. Plane p at a distance 100 mm from origin and plane q at the end of solid arm.

For existing model, at a distance 100 mm from origin, unbalance mass is 2748.269 gram.mm, which is obtained at an angle -68.36973 degree. (i.e. in fourth quadrant) At the end of solid arm unbalance mass is 1366.52 gram.mm, which is obtained at an angle -139.52 degree. (i.e. in third quadrant)

For optimized balanced model, at a distance 100 mm from origin, unbalance mass is 1079.062 gram.mm, which is obtained at an angle 168.4006 degree. (i.e. in second quadrant) At the end of solid arm unbalance mass is 1106.582 gram.mm, which is obtained at an angle -357.2536 degree. (i.e. in first quadrant)

In existing model the location of C.G. is X=0.03690151 mm, Y=0.700903222 mm and Z=-162.4581623 mm and balanced model location of C.G. is X=-0.0119353 mm, Y=0.05802247 mm, and Z=-110.88853 mm. This result shows that balancing of optimized model has been done with greater accuracy then the existing model. So,

there is a reduction in centrifugal force and hence vibration are minimized.

6.3.1 FE Analysis of Optimized Balanced model of Flyer

The FE analysis has been carried out to check modified design of flyer for deformation and von-Mises stresses within operating conditions. The FEA results of deflection and von-Mises stress profiles of original configuration for the flyer is shown in Figure 6.5 and 6.6 respectively. The maximum deflection and von-Mises stress in flyer arm are 2.5093 mm and 53.683 MPa respectively. The FE analysis shows the location of the maximum von Mises stresses near the junction of the arm and the shaft locating hub, as the geometry is constrained near the hub portion. The free end of the flyer arm deflects maximum as that end being the free end. Also the theoretical analysis has been carried out in Chapter 5. The comparison for deflection obtained with theoretical analysis and FE analysis is given in Table 6.3. Table 6.4 shows comparison of results for deflection, maximum von-Mises stresses and weight for existing model and optimized balanced model of flyer.

Table 6.3: Deflection at free end of flyer

Sr.No.	Method	Deflection (mm)
1	Theoretical analysis	2.7
2	FE Analysis	2.5093
3	% reduction	7.062

Table 6.4: Result comparison of existing and optimized balanced model

Sr. No.	Detail of results	Existing model	Optimized balanced model	% reduction
1	Deflection (mm)	2.6574	2.5093	5.573
2	von-Mises stress MPa	53.739	53.683	0.104
3	Weight (kg)	2.07	1.7195	16.93

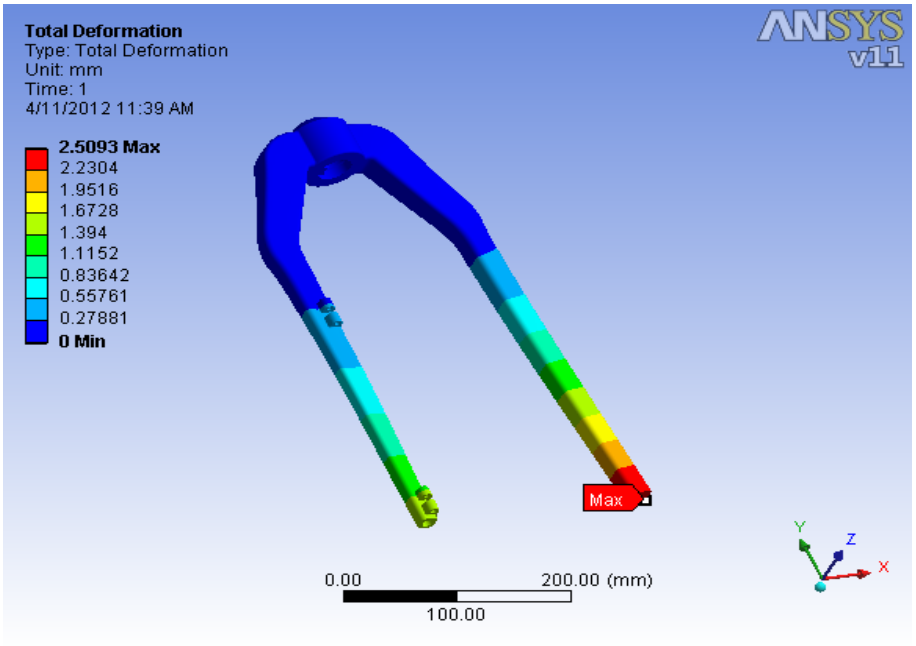

Figure 6.5: Total deformation of optimized balanced model of flyer

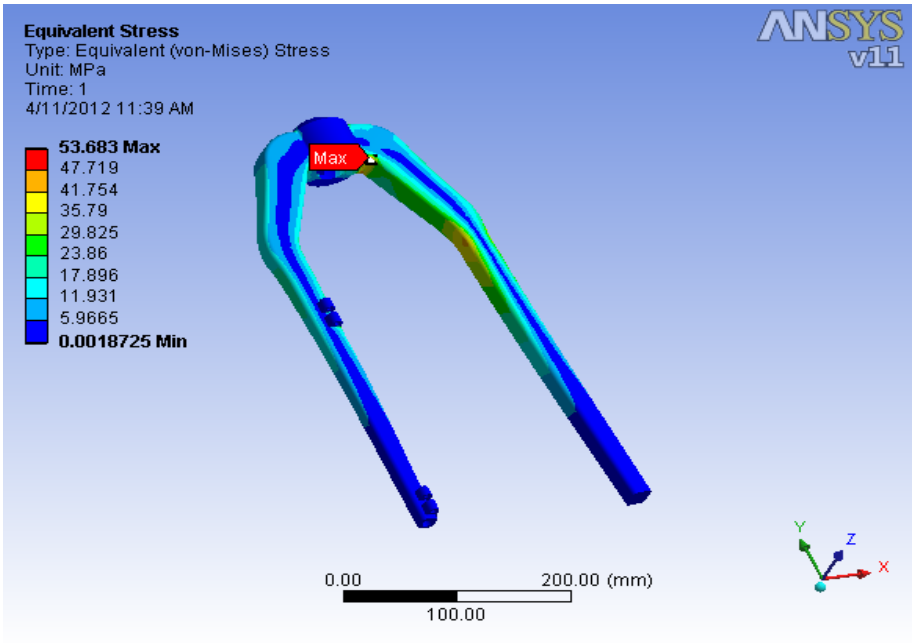

Figure 6.6: Von-Mises Stress on optimized balanced model of flyer

6.4 Drag Force & Coefficient for Proposed Geometry

The value of drag coefficient and drag force for proposed geometry of flyer is 1.24 and 0.764 N respectively. If geometry is changes from aerodynamic shape to rectangle shape, very small amount of drag force is generated which doesn't affect power consumption. Table 6.5 shows the comparisons of drag force with theoretical analysis and FE analysis.

Table 6.5: Drag force for proposed geometry

Sr.No.	Method	Drag Force (N)
1	Theoretical analysis	0.462
2	FE Analysis	0.764
3	% reduction	39.52

6.5 Design for Alternate Material (for optimized balanced model)

The design of flyer have been developed for the five different material. For each material Figure 6.7 shows the comparisons of weight, deflection and FOS. Out of five different material, the aluminium alloy 518 and B390 gives sufficient factor of safety which is greater than three so, this materials can be used for the manufacturing of flyer.

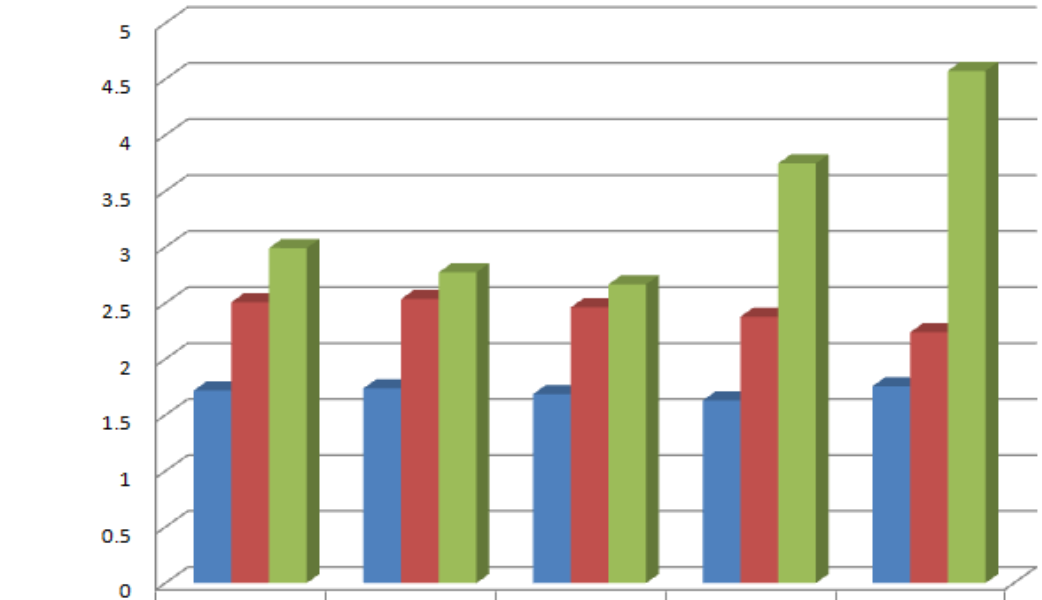

	A380	383	413	518	B390
WEIGHT	1.7187	1.7378	1.687	1.6299	1.7568
DEFLECTION	2.5077	2.5354	2.4614	2.3781	2.2385
F..O.S.	2.99199641	2.774284235	2.667225514	3.746573857	4.573728503

Figure 6.7: Comparison for alternate material

Chapter 7

Conclusion and Future Scope

7.1 Conclusion

The aim of this dissertation is to modified design of the textile machinery component flyer. The new design obtained by size optimization with the help of CAE tool Altair OPTISTRUCT serves the purpose of redesign.

The new optimized design has again being modified for balancing point of view. The optimized balanced design of flyer under existing operational performance gives deflection 2.5093 mm compared to existing design as 2.6574 mm when evaluated using FEA software. Thus the maximum deflection reduces to 5.574%. Also the factor of safety for modified design is grater than three.

The major advantage obtained from redesigning is weight reduction which is about 16.93% from the existing one.

Thus the modification serves the purpose by making the design light weighted but equally strong compared to original one.

7.2 Future Scope

In the present work the emphasis was lead upon reducing the weight of the flyer which will contribute considerably in cost reduction and reduction of the power. It is work

mentioning that there are 120 flyers in a roving frame.
The following points are thought which will further result in efficient operation and manufacturing of flyer.

- Die design for the proposed design to resulting increase the casting yield.
- As per the present practice, the bushes are made from self lubricating material and contribute 10% manufacturing cost of flyer and scope exist for selection of alternative material for the bushes for cost reduction.
- New design of the presser for ease of assembly and manufacturing can be taken up.
- Taken into consideration the functional requirement of the flyer it seems that the existing design which is further being modified in the present work in it self has high inertia an all together a new conceptual light weight design can be thought of.

References

[1] Wills H H, *Copyright By Textile Foundation*, 1937.

[2] Candance Crockeh, *The Complete Spinning Book*, New York Publication, 1977.

[3] http://www.automation.siemens.com/mcms/mc/en/mechanical-engineering/textile-machine/staple-fiber-spinning/ring-spinning-frame/pages/ring-spinning-frame.aspx, July 20 2011.

[4] Harrison P W, *Manual Of Cotton Spinning*, The Textile Institute Butter Worths, Manchester, London, 1964.

[5] Scott William, *Cotton Spinning*, Mac Millan & Co. Limited, London, 1955.

[6] Frederic Herubel Jean, Guebwiller, *Winding-on Flyer for a Roving Frame*, Us Patent 4026097, May 31, 1977.

[7] Novak Peter, Bruno Tanner, *Flyer for Roving Frame*, Us Patent 4377931, March 29, 1983.

[8] Wegger Hans-Peter, Hummel Jorg, Schonfelder Hans-Jurgen, *Flyer Assembly for Roving Frame*, Us Patent 5971091, April 4, 2000.

[9] Carndall H Stephen, Norman Dahl C, *An Introduction to the Mechanics of Solids*, Mc Graw-Hill Book Company, New York, 1976.

[10] Fenner Roger T, *The Mechanics of Solids*, CRC Press, London.

[11] Gere James M, Goodno Barry J, *Mechanics of Materials*, Cengage Learning, Canada.

[12] Bakhtiary N, *A New Approach for Sizing, Shape and Topology Optimization*, SAE International Congress And Exposition, 1996.

[13] Patel Nilesh, Singh Manmohan, *Optimization of Tilt Beam for Reducing Deflection and Material Using HyperMesh/OptiStruct/HyperView FE Package*, Vehicle Research & Development Estt., Ahmednagar.

[14] Torstenfelt B, Klarbring A, *Conceptual Optimal Design for Modular Car Product Families Using Simultaneous Size, Shape and Topology Optimization*, Finite Elements In Analysis and Design, Vol.43, pp.1050-1061, June 2007.

[15] Sonmez Fazil O, *Shape Optimization of 2d Structures Using Simulated Annealing*, Comput. Methods Appl. Mech. Engg. Vol.196, pp.3279-3299, January 2007.

[16] *Fundamental of balancing*, Third Edition, April 1990.

[17] Sharma C S, Purohit Kamlesh, *Theory of Mechanism and Machines*, Prantice Hall of India Private Limited, New Delhi 2006.

[18] Singh Sadhu, *Theory of Machines*, Pearson Education, Dorlling Kindersley Private Limited, New Delhi.

[19] http://www.wikipedia.org/wiki/drag-coefficient, March 25 2012.

[20] http://www.pbs.org/mova/space/lift-drag.htm, March 26 2012.

[21] *Casting*, ASM Handbook, Ninth Edition, Vol.15, pp.492-537.